# The Comprehensive AOCMF Classification System: Midface Fractures - Level 3 Tutorial

Carl-Peter Cornelius, MD, DDS[1] Laurent Audigé, DVM, PhD[2,3] Christoph Kunz, MD, DDS[4]
Carlos H. Buitrago-Téllez, MD[5] Randal Rudderman, MD, FACS[6] Joachim Prein, MD, DDS[4]

[1] Department of Oral and Maxillofacial Surgery, Ludwig Maximilians Universität München, Germany
[2] AO Clinical Investigation and Documentation, AO Foundation, Dübendorf, Switzerland
[3] Research and Development Department, Schulthess Clinic, Zürich, Switzerland
[4] Clinic for Oral and Craniomaxillofacial Surgery, University Hospital Basel, Basel, Switzerland
[5] Imaging Center Aarau, Institute of Radiology Zofingen Hospital, Zofingen, Switzerland
[6] Plastic, Reconstruction & Maxillofacial Surgery, Alpharetta, Georgia

**Address for correspondence** Carl-Peter Cornelius, MD, DDS, Department of Oral and Maxillofacial Surgery, Ludwig Maximilians Universität, Lindwurmstrasse 2A, D-80337 München, Germany (e-mail: peter.cornelius@med.lmu.de).

Craniomaxillofac Trauma Reconstruction 2014;7(Suppl 1):S68–S91

## Abstract

This tutorial outlines the details of the AOCMF image-based classification system for fractures of the midface at the precision level 3. The topography of the different midface regions (central midface—upper central midface, intermediate central midface, lower central midface—incorporating the naso-orbito-ethmoid region; lateral midface—zygoma and zygomatic arch, palate) is subdivided in much greater detail than in level 2 going beyond the Le Fort fracture types and its analogs. The level 3 midface classification system is presented along with guidelines to precisely delineate the fracture patterns in these specific subregions. It is easy to plot common fracture entities, such as nasal and naso-orbito-ethmoid, and their variants due to the refined structural layout of the subregions. As a key attribute, this focused approach permits to document the occurrence of fragmentation (i.e., single vs. multiple fracture lines), displacement, and bone loss. Moreover, the preinjury dental state and the degree of alveolar atrophy in edentulous maxillary regions can be recorded. On the basis of these individual features, tooth injuries, periodontal trauma, and fracture involvement of the alveolar process can be assessed. Coding rules are given to set up a distinctive formula for typical midface fractures and their combinations. The instructions and illustrations are elucidated by a series of radiographic imaging examples. A critical appraisal of the design of this level 3 midface classification is made.

**Keywords**
- fracture classification
- central and lateral midface
- zygoma
- tooth injuries

The AOCMF craniomaxillofacial fracture classification system was developed in the form of a hierarchical three-level system with increasing details and complexity.[1] Within the midface, the level 2 system describes the location of the fractures within defined regions in the central and lateral midface with reference to classic Le Fort fractures and its analogs.[2]

The facial skeleton is composed of multiple singular or paired bones that are articulated by fixed sutures. The overall framework is subdivided into a few major topographical regions predisposed to typical fracture entities (e.g., naso-ethmoidal, naso-maxillary, dentoalveolar, and zygomatico-orbital). The precision level 3 midface fracture classification adds a new layer of elaboration going beyond the basic level 2


AOCMF
Clavadelerstrasse 8
7270 Davos
Switzerland
Tel: +41 44 200 24 20.

**DOI** http://dx.doi.org/10.1055/s-0034-1389561.
**ISSN** 1943-3875.

topographic assessment in these subregions in more detail. Fragmentation, displacement, and bone loss are the descriptors to refer to fracture morphology within these layouts. Rules for coding the fracture location and the morphologic variables are established.

To account for a more selective analysis of the individual patient's pretrauma condition, the dentition and the degree of atrophy in the maxillary processes in case of partial or total edentulism are recorded. These features serve as a baseline to document tooth injuries, periodontal trauma, and alveolar process fractures. A series of case examples with clinical imaging points out the modalities of this midface level 3 classification. It is recommended to revisit the midface level 2 tutorial[2] briefly before passing on.

## Level 3 Midface Fracture Classification System

The midface level 3 classification system is introduced in the following sections covering specific anatomical subregions of the central and lateral midface.

### Central Midface

The central midface includes three horizontal partitions labeled LCM (lower central midface), ICM (intermediate central midface), and UCM (upper central midface), which are used in a building block concept to synapse Le Fort I and Le Fort II fractures in level 2.[2]

Fracture morphology in the central midface is documented by fragmentation, displacement, and bone loss. The fragmentation within the partitions is determined by the number of fracture lines as 0 = nonfragmented (single straight or twisted fracture line) or 1 = fragmented (more than a single fracture line). So-called multifragmentary or, in outmoded parlance, comminuted fractures, representing fractures in which bone is shattered, splintered or crushed into many pieces, are included in the latter category. Displacement is attested whenever the fragments have moved out of their original location and lack alignment to the skeletal superstructure regardless of the metric amount. Traumatic bone loss, also referred to as bone defect (d), applies to deficits ranging from small fragments to large sections. Without distinction of the potential spectrum of the deficit, it is either negated (0 = no bone loss) or affirmed (1 = bone loss).

The UCM, formed by the nasal skeleton and the medial orbital rims, is subdivided into medial and lateral subregions (►**Fig. 1**). The medial or central part consists of the paired nasal bones. The nasal bones are interposed above the nasal aperture between the frontonasal maxillary processes that form the nasal sidewalls and medial orbital rims conjointly. The nasal septum encompasses three components: the quadrangular cartilage, the perpendicular plate of the ethmoid, and the vomer. In loose accordance with the height of the vomer and the perpendicular plate, the entire septal structure is arbitrarily subdivided along its vertical extent into two halves, the upper and lower septum. Unilateral or bilateral fractures of the nasal skeleton can be recorded by specifying the involved UCM subdivisions.

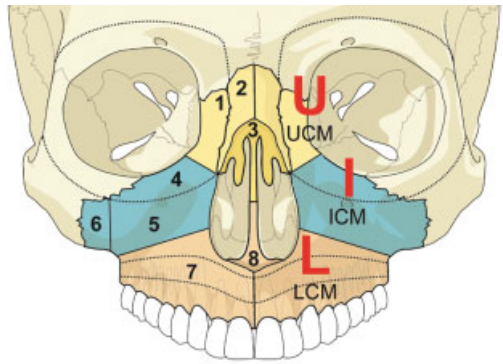


**Figure 1** Central midface subdivisions. UCM, upper central midface: 1, frontonasal maxillary process/medial orbital rim; 2, nasal bone; 3, upper nasal septum/ethmoidal perpendicular plate; ICM, intermediate central midface: 4, medial part of the inferior orbital rim (i.e., infraorbital margin of the maxilla—the entire orbital rim is marked as a band-like outer ring around the orbital opening); 5, anterior antral wall and parapiriform buttress; 6, area of zygomatico-maxillary crest (ZMC)—ICM part; LCM, lower central midface: 7, maxillary alveolar process with two reference lines indicating potential degrees of atrophy in edentulism; 8, lower nasal septum/vomer. The division line between UCM and ICM coincides with the demarcation between the medial and the inferior orbital rim in the inferomedial quadrant.

### Naso-orbito-ethmoid Fractures

In addition to nasal fracture components naso-orbital-ethmoid (NOE) fracture entities typically involve the internal orbit, the lacrimal bone, and ethmoid.[3,4] The frontal bone and intracranial structures may be affected too. To detail the extent and fragmentation in the overall or en bloc NOE fracture pattern,[2] all concomitant structures are delineated in the level 3 graphic representations,[5] not only of the midface, but also in the orbit[6] documentation systems. The extent of the fractures, including the canthal ligament-bearing or "central" fragment (level 3 orbit,[6] ►**Fig. 2** and Table 2) can be indirectly specified by indicating if the frontonasal maxillary processes and the anterior section of the medial orbital wall (i.e., the lacrimal bone) are involved or not. A true avulsion of the medial canthal ligament insertion from the "central" fragment of the medial orbital rim and lacrimal bone needs clinical and/or intraoperative physical assessment, however, and is not amenable to preoperative radiographic analysis.[7–14] A posterior intrusion of the nasal pyramid and lateral displacement of the NOE fragments resulting in a flattened and short nasal bridge, telecanthus, and rounding of the palpebral fissures is accessible both to physical examination and imaging. However, at this time (i.e., AOCOIAC version 4.0[5]) the specification and grading of fragment displacement (e.g., asymmetric) in the central midface is not optimized for a standardized documentation purpose.

The UCM and ICM in combination can be brought into line with the blueprint of the classical Le Fort II central midface fracture in its antero superior extent. The ICM corresponds to the midportion of the central midface pyramid and encompasses the medial part of the inferior orbital rim, the facial antral wall, and para piriform buttress.[2] Involvement of the ICM can be further specified by whether the inferior orbital

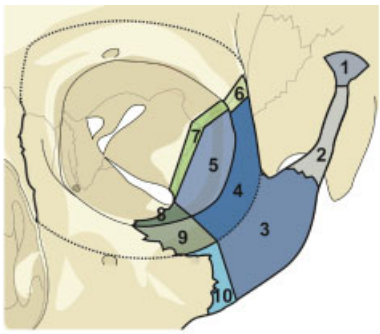


| Level 3 zygoma system (92 Z) | | Associated codes | |
|---|---|---|---|
| ID | Subregions | Level 2 | Level 3 Orbit |
| 1 | Temporal origin of the zygomatic arch | Z | |
| 2 | Zygomatic arch | Z | |
| 3 | Zygomatic body | Z | |
| 4 | Zygomatic body (lateral orbital rim) | Z | Rl |
| 5 | Anterior part of lateral orbital wall | Ol | W1l |
| 6 | Area of zygomaticofrontal suture | Z | Rl |
| 7 | Area of zygomaticosphenoidal suture (Greater wing of sphenoid) | Ol | W1l |
| 8 | Zygoma part of anterior part of inferior orbital wall | Oi | W1i |
| 9 | Zygoma part of inferior orbital rim (infraorbital rim) | Z | Ri |
| 10 | Area of zygomaticomaxillary crest—Zygoma part | Z | |

**Figure 2** Zygoma subregions. Z, zygoma; Rl, lateral orbital rim; Ri: inferior orbital rim (infraorbital rim); W1, anterior part of orbital wall.

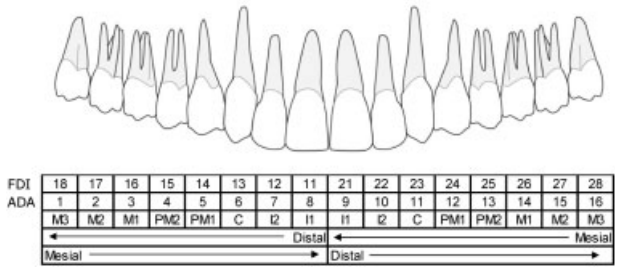


**Figure 3** Upper dentition, FDI dental formula, ADA tooth numbering, and tooth acronyms. FDI (Fédération Dentaire Internationale) tooth numbering formula (adapted by WHO) for permanent teeth is referred to by a two-digit number, one for the quadrant and the other for the tooth order from mesial to distal. In the tooth numbering formula of the ADA (American Dental Association), the teeth are marked with consecutive numbers following a clockwise order beginning with the maxillary right third molar (1) and continuing to the mandibular right third molar (32). Individual teeth or teeth groups are often acronymed: "I" stands for incisors, "C" for canine, "PM" for premolar, and "M" for molar. To avoid confusion, two terms used conventionally in the dental nomenclature merit clarification: mesial—means toward the midline; distal—means away from the midline Note: In surgical terminology, distal is the antonym of proximal and means "away from the center," which is toward the midline.

rim (►**Fig. 1**, ID 4) is involved or not. In addition, if a fracture line follows the course of the zygomatico-maxillary suture, it can be classified as either an ICM or a zygoma fracture, or even both with respect to the predominating or all-encompassing fracture pattern (►**Fig. 1**, ID 6 and ►**Fig. 2**, ID 10). The LCM matches with the Le Fort I level. Accordingly, the LCM includes the solid body of the maxilla, the maxillary tuberosity, and the upper alveolar processes of the maxilla, which enclose the sockets and the roots of the upper teeth.[2] Instead of subdividing the LCM into further topographical subregions, the fracture involvement of the alveolar process is used to detail additional fracture zones in the inferior maxillae.

## Dentition

The nomenclature to describe the dental sequelae of a midfacial injury follows the same scheme as used in the level 3 system for mandibular fractures.[15]

The FDI (Fédération Dentaire Internationale) two-digit tooth numbering formula for permanent teeth is used to register the likely preinjury dental status (absent teeth before trauma) (►**Fig. 3**).

## Edentulism—Degree of Maxillary Atrophy

Over time, the alveolar ridge of any edentulous portion in the anterior and posterior maxilla will be gradually resorbed and remodeled with subsequent reduction of height.[16] In case of partial or complete edentulism, three stages of bony atrophy or alveolar ridge height are defined for the left and right maxilla (►**Fig. 4**):

- 0 = No or mild atrophy vertical height $\geq$ 11 mm
- 1 = Moderate atrophy vertical height 6–10 mm
- 2 = Severe atrophy vertical height $\leq$ 5 mm.

In the posterior maxilla, coronal computed tomographic (CT) scan sections are most appropriate for the evaluation of the height of the alveolar ridge relative to the extent of the maxillary sinus (distance between the alveolar crest and floor of the maxillary sinus). In the anterior maxilla, the vertical dimension of the alveolar ridge (distance between the crest and the nasal floor) is best assessed in sagittal CT scans. For each side, the most severe occurring atrophy is considered.

## Tooth Injuries/Periodontal Trauma

Periodontal and dental hard tissue injuries are documented separately for each tooth involved by the trauma with regard to tooth loss (tooth avulsion) or the occurrence of tooth injuries (i.e., crown and/or root fractures and tooth loosening).[17]

- *Tooth avulsion/tooth loss/missing teeth*: the tooth is completely luxated out of its socket. Radiographs show an empty socket.
- *Crown and/or root fractures*: These injuries include enamel fractures (confined to the enamel), enamel-dentin-pulp fractures (substantial loss of tooth substance), crown-root fractures (involving both the coronal and intra-alveolar parts of the tooth), and root fractures (only within the intra-alveolar part).
- *Tooth loosening*: Without displacement, the only sign and symptom is a marked tenderness to percussion and "a sore tooth." On radiographs, the injured tooth is in its normal position in the socket; however, loosening can be indirectly ascertained because of widening of periodontal spaces

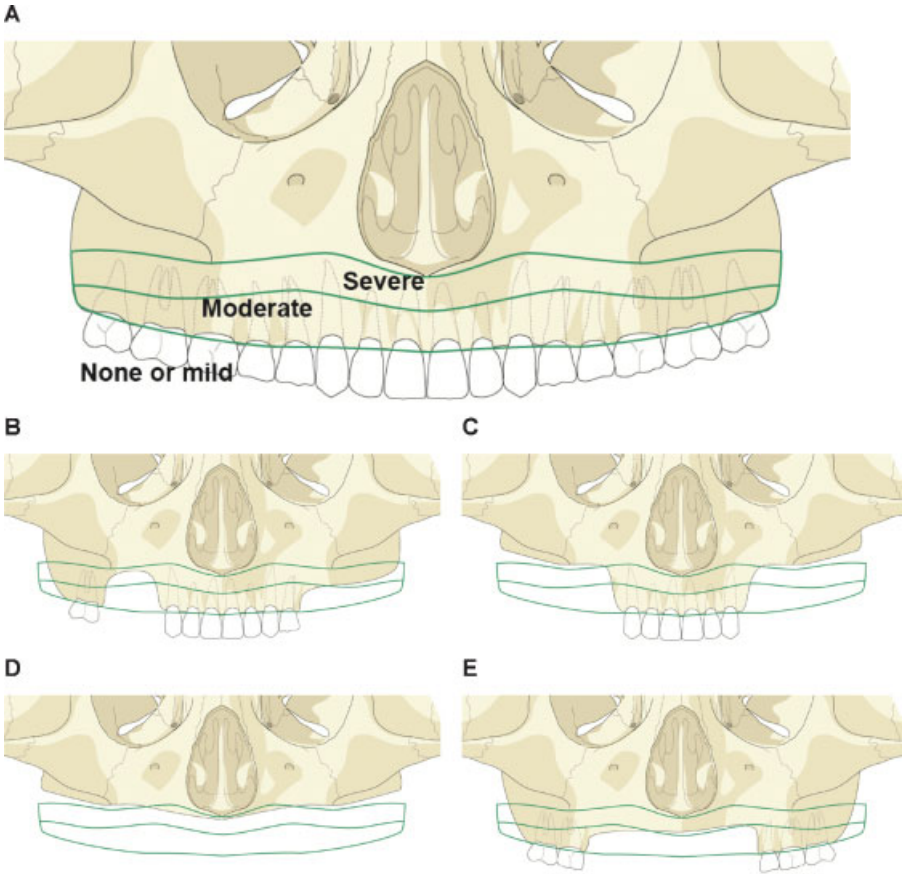


**Figure 4** Illustration of maxilla edentulism and atrophy. (A) "atrophy grid" superimposed on a fully dentulous maxilla with permanent teeth. Three stages of atrophy are defined: 0 = no atrophy, original height of the maxilla preserved, or mild atrophy; 1 = moderate atrophy; and 2 = severe atrophy associated with loss of alveolar processes; – the atrophic region is identified by the missing teeth; (B) moderate level of atrophy (stage 1) on the left side of the patient, and severe atrophy (stage 2) on the right side; (C) severe level of atrophy (stage 2) in both premolar and molar regions; (D) complete edentulism with severe atrophy; and (E) partial central edentulism with bilateral moderate atrophy.

mesially or distally. When displaced also, the tooth suffers partial axial shifting out of its socket (extrusion).

If there is suspicion for tooth injuries or loss, the nature of which cannot be further clarified (e.g., due to imaging shortages), these are classified under the category "undetermined." The lower dentition is addressed in the tutorial paper for level 3 mandible.[15]

### Fracture Involvement of the Alveolar Process

Alveolar process fractures are documented similarly to the mandible.[15] The FDI numbers of the involved teeth are indicated to provide information about the location and extent of the fracture. The exact course of the vertical fracture lines comprising the involved teeth, however—directly through the tooth sockets, through the adjacent periodontal ligaments, or the bony interdental spaces—may differ on either side of the block-shaped alveolar fragment and is not specified in detail.

If an edentulous region of the alveolar process is involved, the vertical boundaries are indicated as if the teeth were there. The horizontal fracture line may cross over the tooth apices or lie at or below their level. If the upper fracture line traverses through the anterior wall of the maxillary sinus, the palate, and/or the nasal floor, the alveolar process fracture is documented in combination with a fracture of the LCM and/or a palatal fracture.

### Palate

The palatal shelves consist of the premaxilla, the palatine processes of the maxilla, and the horizontal plate of the palatine bone. Fractures of the palate are classified into one of three categories: 1 = one transverse fracture line; 2 = one para- or mid-sagittal fracture line; 3 = two or more fracture lines. The occurrence of bone loss (d = bone defect) can be indicated also.

### Pterygoid Process

The pterygoid processes are regarded as self-contained anatomical regions and not as parts of the sphenoid bone. Each pterygoid process can be classified as fractured. In addition, as a fracture morphology feature, it is determined whether the process is separated vertically from the maxilla (LCM/ICM) or not.

### Lateral Midface (Zygoma)

The zygoma and its anatomical subregions constitute the lateral midface attached to each side of the maxillary portions of the central midface pyramid in transition to the greater

sphenoid wing, the frontal bone, and the temporal bone. In the level 2 midface classification system, the zygoma and the zygomatic arch have been addressed as a single anatomic region.[2] The zygomatic arch extends from the temporal process of the zygoma to the zygomatic process of the temporal bone (►**Fig. 2**). The fossa of the temporomandibular joint (mandibular fossa) is incorporated into the temporal origin of the zygomatic arch (subregion ID 1). In front of the mandibular fossa, the anterior root of the zygomatic process emerges medially from the articular tubercle. This anterior root concurs with the anterior border of the temporal origin of the zygomatic arch.

Five articulations extending from the body of the zygoma connect to the adjacent bones (►**Fig. 2**):

- Frontal process or lateral orbital rim (subregion ID 4)
- Zygomaticomaxillary buttress or zygomaticomaxillary crest (ZMC; subregion ID 10 and Fig. 1 subregion ID 6)
- Inferior orbital process of the zygoma (subregion ID 9)
- Lateral orbital process (facies orbitalis or zygomaticosphenoid flange) of the zygoma (= anterior portion of the lateral orbital wall/subregion ID 5)
- Temporal process continuous with the zygomatic arch (subregion ID 3).

The prolongation of the inferior orbital fissure beyond its anterior loop provides a clear demarcation between the inferior and lateral orbital surface of the zygoma (►**Fig. 2**, subregions ID 8, 9, and 10 vs. subregions ID 3, 4, 5, and 7). A line running parallel around the orbital rim through the midpoint of the curvature between zygomatic arch and the frontal process (= outer demarcation line of the orbital rim circumference) identifies the orbital rims inferiorly and laterally (subregions ID 9 and 4). The posterior limit of the zygomatic body is made up by the zygomaticotemporal suture line. The inferior limit of the zygomatic body is given by the caudal bony crest traversing into the zygomaticomaxillary buttress. The infraorbital process of the zygoma

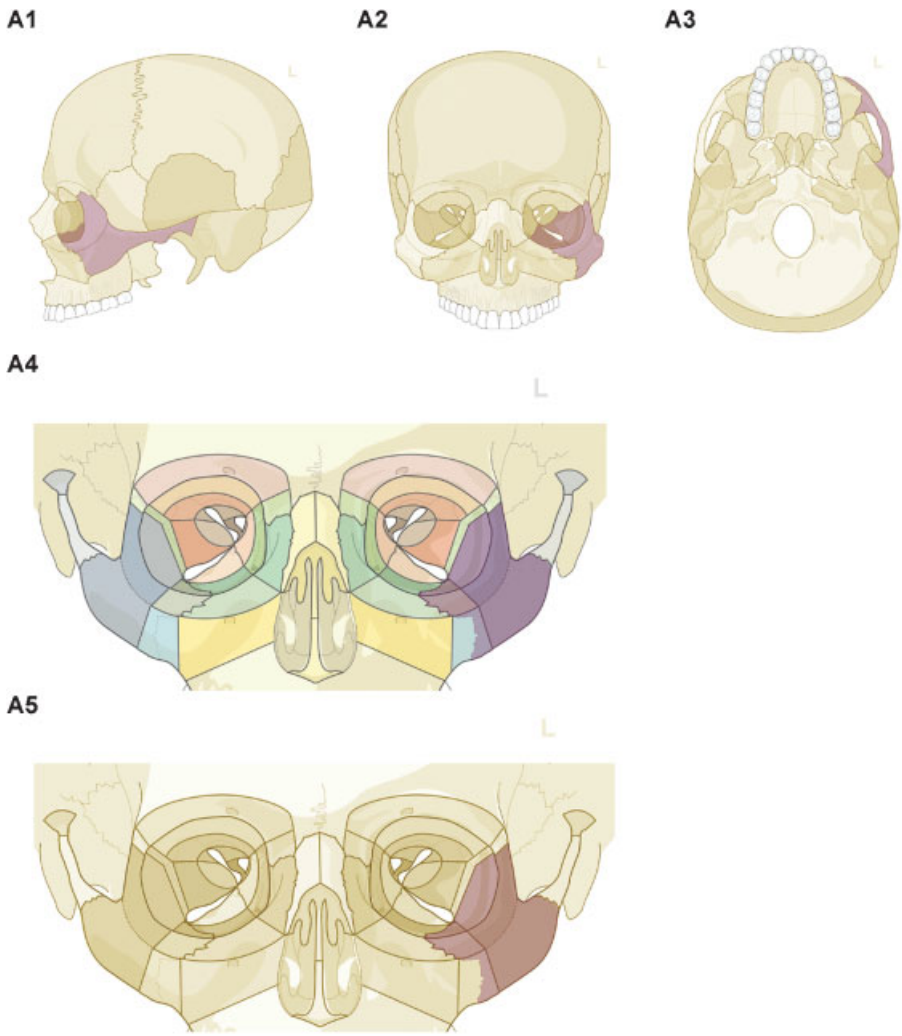


**Figure 5** Zygoma/zygomatic arch ensemble—roadmap for charting fractures of increasing complexity and topographical extent. (A1–A5) En bloc zygoma fracture: shortcut marking—skull icons (A1–A3) and panoramic midface/orbits icon, color mode display (A4), black and white mode display (A5).

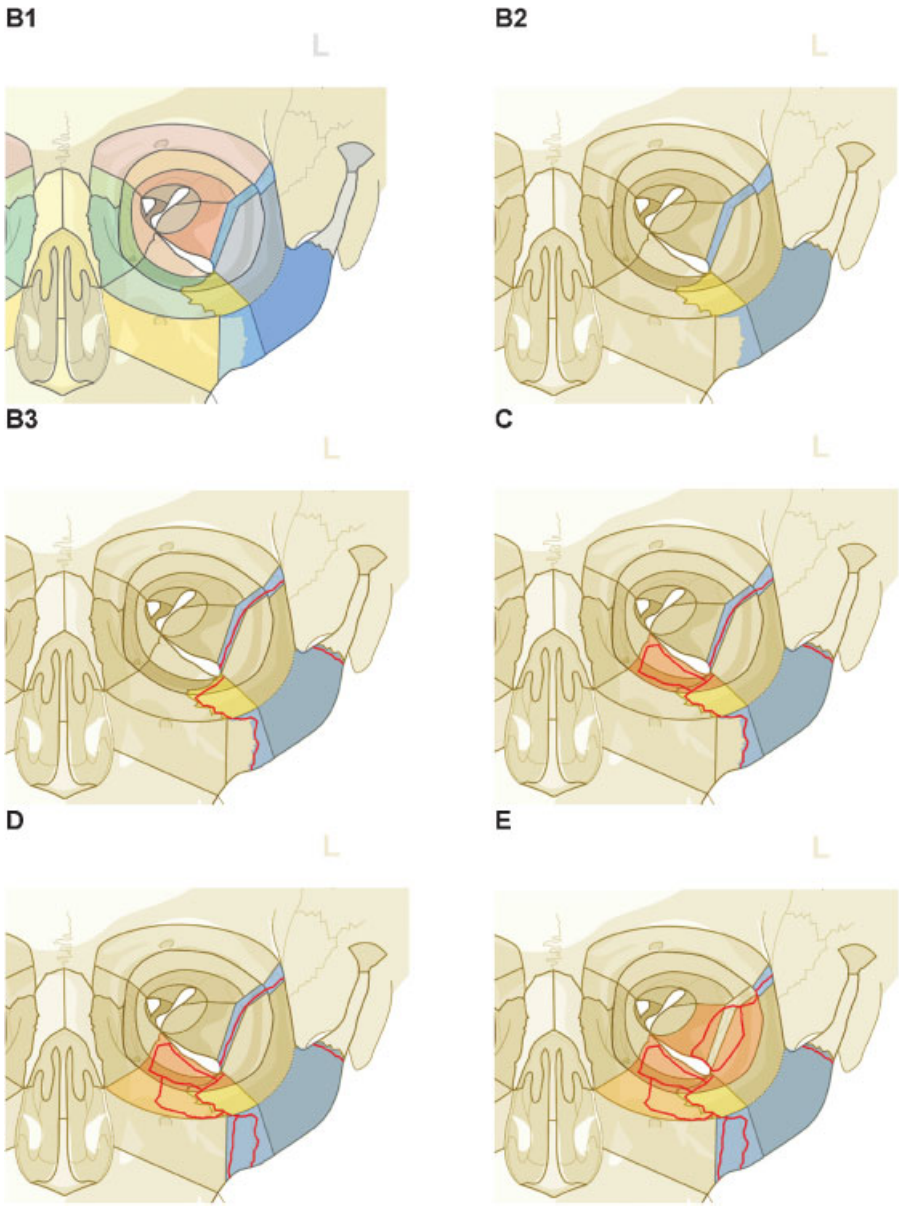


**Figure 5** (*Continued*) (B1–B3) En bloc zygoma fracture: composition of separately marked subregions—color mode display (B1), black and white mode display (B2), marked fracture lines (red) additionally sketched (B3). (C) En bloc zygoma fracture (¼ B3) associated with a lamellar displaced orbital floor fracture (orange). (D) Multiple fracture lines at ZMC (ICM part and zygoma part) plus intermediate fragment along the infraorbital rim (ICM part) in addition to fractures displayed in (C). (E) Lamellar fracture in the lateral orbital wall running through greater wing of the sphenoid (¼ midorbit lateral wall) and the anterior flange of the zygoma (anterior lateral orbital wall) in addition to fractures displayed in (D). As the course of the fracture lines bypasses the ZSS it is left blank.

(subregion ID 9) stretches between the lower border of the lateral orbital rim and the zygomaticomaxillary suture. The area of the ZMC (Fig. 2 subregions ID 10 and Fig. 1 subregion ID 6) is situated just below the inferior limits of the infraorbital process and the anterior limit of the zygomatic body. The ZMC area incorporates the lower part of the zygomaticomaxillary suture line, which divides it vertically into a lateral zygoma part (Fig. 2 subregion ID 10) and a medial ICM part (Fig. 1 subregion ID 6). The lateral orbital process of the zygoma is continuous with the orbital roof and blends with the zygomatic process of the frontal bone (lateral orbital rim) superiorly. The zygomaticofrontal suture (ZFS) line (labeled as subregion ID 6) conjoins these merging bony portions. The zygomaticosphenoid suture (ZSS) line (labeled as subregion ID 7) abuts the posterior margin of the lateral orbital process of the zygoma to the anterior edge of the greater wing of the sphenoid.

At present (i.e., AOCOIAC version 4.0[5]), the full spectrum of fracture morphology in terms of fragmentation, displacement, and bone loss is applicable only in the two subregions of the zygoma constituting the inferolateral orbital rim (ID 4 and 9). The description of the fracture morphology at the

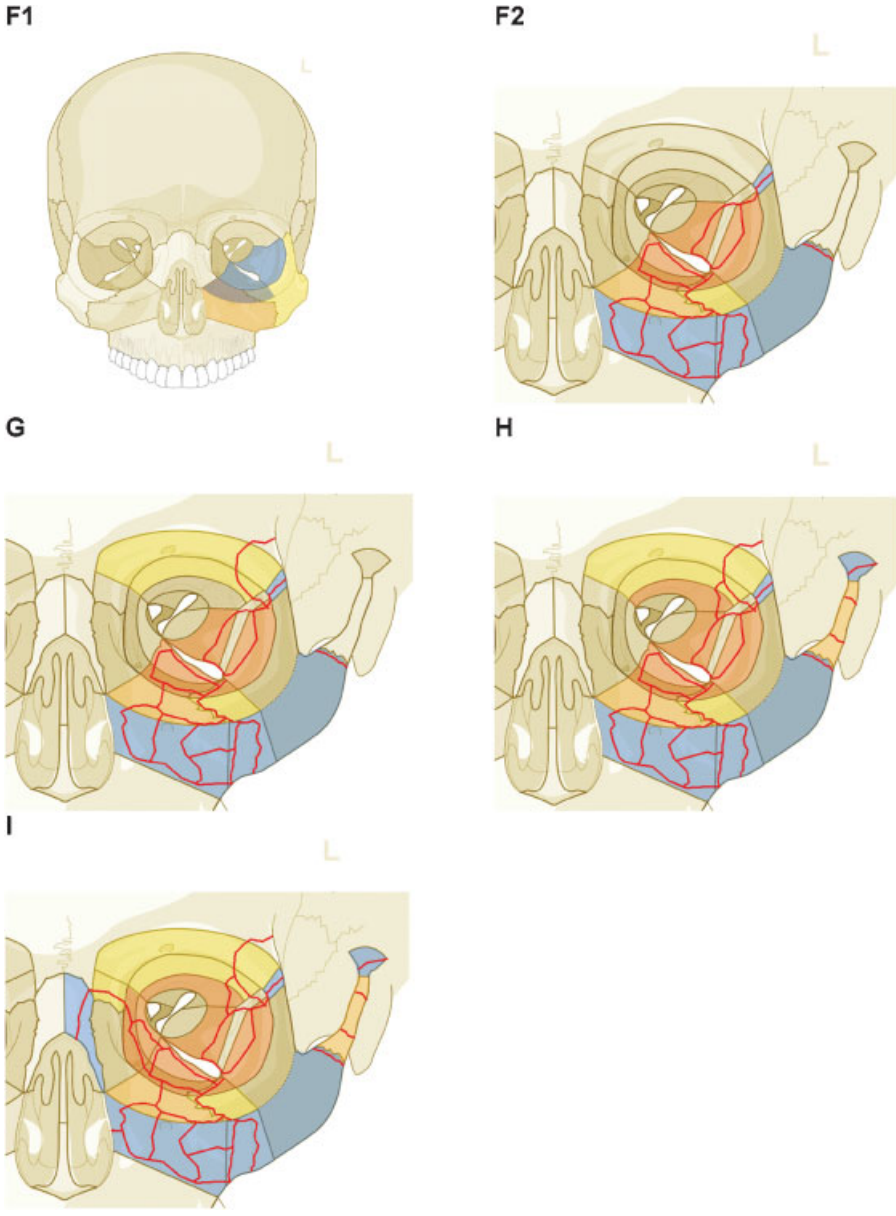


**Figure 5** (*Continued*) (F1, F2) Multifragmentation of the antral wall of the maxillary sinus (ICM) in addition to the fractures displayed in (E). In the present AOCOIAC version fragmentation, displacement and bone loss can be indicated in the skull icons only (F1—orange subregion), in the panoramic midface/orbits icon it is marked as fractured (F2—blue) as a backlink. (G) Crack of the zygomatic process of the frontal bone (superior orbital rim) in conjunction with the lateral edge of anterior superior orbital wall in addition to fractures displayed in (F2). (H) Multiple fragments of the zygomatic arch and shearing fracture of the temporal origin in addition to fracture displayed in (G). (I) Lamellar fracture of the anterior superior orbital wall in the superolateral quadrant, a fracture line running through the piriform rim in the ICM, a unilateral naso-orbito-ethmoidal fracture through the nasal bone, the nasofrontal process, and a lamellar fracture of the medial orbital wall in addition to fractures displayed in (H). These complete an entity which is analogous to a unilateral or hemi Le Fort I, II, and III fracture. Note: Color coding of a subregion, blue denotes the presence of a fracture without any further differentiation, yellow stands for nonfragmented, nondisplaced, orange is the equivalent for fragmented, a gray crosshatching points out a bone loss. The fracture morphology features in the subregions of the graphical schemes are set to "nondisplaced," and "no bone loss" wherever applicable. Other entries will alter the color code in correlation to the individual scenario of the injury. The subregions can be affected in various arrangements and different formations. The shown incremental order represents a random selection and intends to chart a comparable roadmap to classify distinctive midface injuries.

lateral and inferior orbital flanges of the zygoma (ID 5 and 8) conforms to the precepts and nomenclature allocated to the orbital walls within the level 3 Orbital Fracture Classification.[6]

The ZFS line (ID 6) and ZSS (ID 7) are marked to indicate that the course of fracture lines follows straightway to these sutures. Intermediate fragmentation into the adjacent subregions, such as the lateral orbital flange of the zygoma and/or the greater wing of the sphenoid or the zygomatic process of the frontal bone, is specified as fragments within these respective sites. ZFS and ZSS are left unmarked then.

The zygomatic body (subregion ID 3) and the area of the ZMC (subregion ID 10 and Fig. 1 subregion ID 6) do not hold

specific features to further characterize fracture morphology. An auxiliary pathway to assign these features is provided for the zygoma in total.

As the antral walls are a principal part of the ICM, the fracture morphology features can be accessed through the ICM pull-down menus in the respective skull views. These pull-down menus contain a list of level 2 and level 3 features.

Plural fracture lines and multifragmentation within a specific sector of the circular orbital rim can be highlighted with a dark background by activating its anatomic designation (e.g., inferior rim, lateral rim, medial rim, and superior rim) in the pull-down menus in the respective region (ICM and/or zygoma, zygoma, ICM and/or frontal bone) within the skull views. This classification, however, is not automatically transferred into the various subregions around the orbital cavity in the more precise panoramic midface/orbits view.

### Zygoma Fracture Pattern Catalog

In routine clinical parlance, fracture patterns are addressed in a concise way for rapid communication. This is reflected in the on-going practice to wrap up central and centrolateral midface fractures into terms analogous to classic Le Fort fracture types.

For the same purpose, the infinite number of variants under the heading of the zygoma/zygomatic arch fractures requires a few basic categories to channel a standardized classification approach. Accordingly, the enormous choice of options given by the level 3 grid of 10 subregions constituting the zygoma/zygomatic arch bone ensemble (►**Fig. 2**) and their fracture morphology features needs to be caught in a few default settings or graphic prototypes (►**Fig. 5**), on which to compile a catalog of permutations in multicentre agreement studies upcoming in the future (1).

Such a default configuration is an isolated en bloc zygoma fracture with single fracture lines passing through the sutures at its five anatomic articulations. This en bloc zygoma fracture can be marked in the menu bars of the skull view, what will be responded with an intense magenta coloration of the zygoma including the complete lateral wall of the orbit as is characteristic for level 2 (►**Fig. 5A**). There is upward and downward functionality for en bloc zygoma fractures between level 2 and level 3. So, the shortcut activation is simultaneously displayed in the panoramic midface/orbits view, however, the involvement of the lateral orbital wall is automatically restricted to the orbital flange of the zygoma (►**Fig. 5B**). By definition, the en bloc zygoma fracture does not exhibit noteworthy intermediate fragments. Therefore, displacement of the monobloc is the only recordable morphology feature in the skull-view menu bar.

An alternative pathway to outline the en bloc zygoma fracture prototype is to select the subregions separately. The graphical scheme of such an assembly will have a different look and color scheme (►**Fig. 5B** and **C**), but it provides a roadmap to capture and classify fractures of increasing complexity owing to plural fractures and involvement of adjoining topographical regions. In a systematic process, the subregions of the zygoma/zygomatic arch ensemble and its vicinity can be labeled as fragmented or/and displaced with or without bone loss to account for any increments in the magnitude of the respective fracture pattern (►**Fig. 5**).

### Fracture Coding and Topographical Distribution

Fractures of the midface are identified with the two-digit code 92[1] followed by a letter identifying the involved divisions. Regarding the more detailed fracture topography and fragmentation in the level 3 system, each involved region is further coded indicating the fragmentation (0 = not-fragmented; 1 = fragmented) and the letter "d" in case of bone loss (defect). Fracture displacement within the zygoma and zygomatic arch can be documented; however, it is not included in the overall code.

The regions are coded in the order from the patient's right side to the patient's left side starting with the zygoma. In the overall fracture code, the small letter "m" (abbreviation for "middle"), or the letter "U" if the upper midface division is fractured, marks the limit between the two sides. Contrary to fractures in the mandible, it is not documented if a fracture line is contiguous between two involved subdivisions.

Hence, for example, the code 92 Z0.I1.U1.I0 refers to a midface injury on the right side involving a single fracture line (nonfragmented fracture) in the zygoma, multiple fracture lines (fragmented fracture) in the ICM and UCM, and a nonfragmented fracture in the ICM on the left side.

## Discussion

This level 3 classification for midface fractures intends to build up on and optimize existing schemes. It is focused on a detailed description of topographical regions and subregions and their fracture involvement in terms of fragmentation, bone loss, and displacement. Most existing classification systems generally rely on visual pattern recognition with depiction of various types.[8,18–31] The fracture pattern identified by the surgeon is matched to the best available illustration in the accompanying graphical schemes. This method is fraught with imprecision, in particular, if complex fracture patterns are evaluated. Nonetheless, it is taken for granted that different examiners go for a similar choice with limited concerns about any associated risk of misclassification.

This level 3 midface classification involves determining the fracture involvement of individual regions and the subregions of the LCM, ICM, UCM (►**Fig. 1**), zygoma, and zygomatic arch (►**Fig. 2**).

Fragmentation is one of the features of fracture morphology.[15] The term has different meanings and covers diverse bone conditions in a fracture zone from structurally intact (nonfragmented) to smashed into bits and pieces (fragmented). The attribute "fragmented" or "multifragmentary" in the context of this level 3 midface classification is assigned to fractures with more than one fracture line resulting in three or more pieces.

Nonetheless, it becomes clear that "fragmentation" does not equate with "comminution" or its current substitution "multifragmentation." Fragmentation in the proposed system

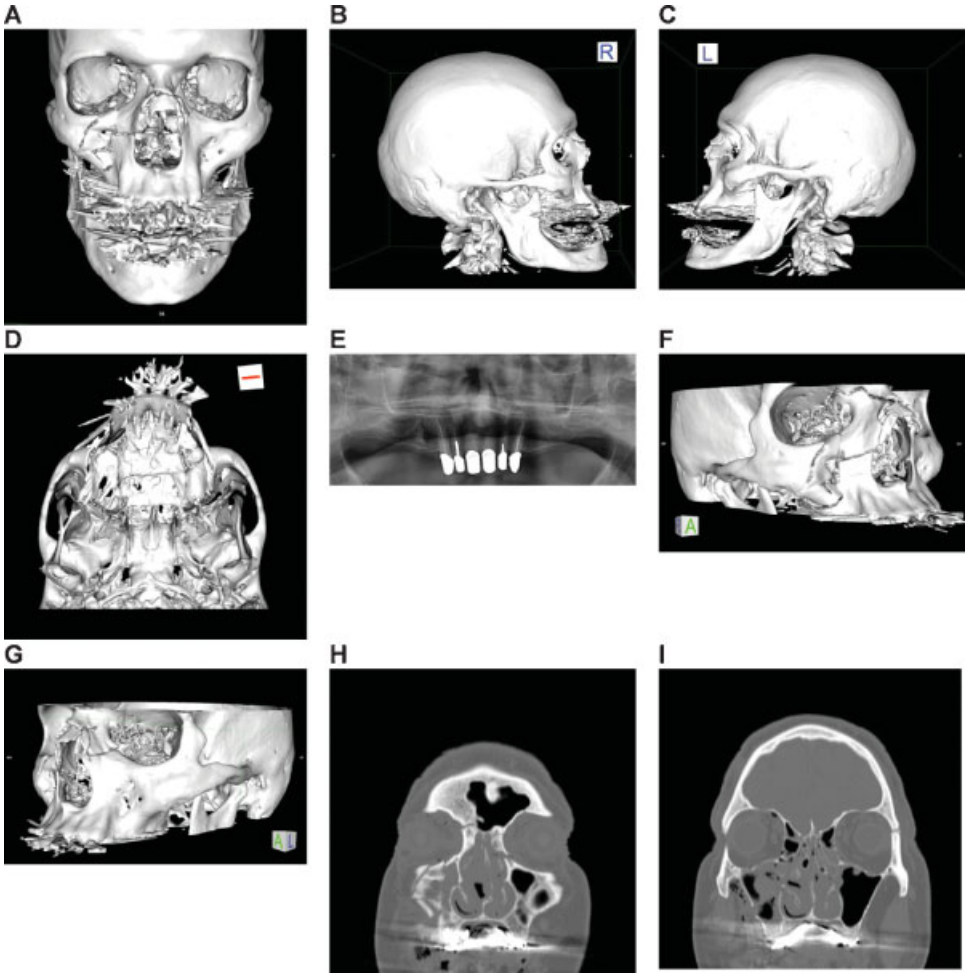


**Figure 6** Asymmetric Le Fort Level midface fracture. Three-dimensional (3D) computed tomographic (CT) scans— (A) frontal view, (B) lateral view right, (C) lateral view left, (D) basal view—mandible removed; (E) panoramic X-ray–OPT; (F, G) 3D CT scans—oblique views, right,left (H, I) coronal CT scans.

is determined by selecting between the two alternatives "nonfragmented" versus "fragmented" in each midface region defined according to the presence of single or multiple fracture lines. Fragmentation must be distinguished from the overall fracture pattern, which refers to the distribution and number of fractures over the regions in the entire midface.

There is a close interrelationship between the fracture components and the displacement of midface fractures (►**Figs. 6–11**). With the intention to give treatment recommendations, Manson et al[32] related fractures with little comminution and displacement to "Low Energy" trauma, moderately comminuted injuries with mild to marked displacement to "Middle Energy," and a high degree of fragmentation, displacement, and instability to "High Energy" trauma. Fragmentation occurs in an abundant variety depending on the distribution, number, and size of fragments. Displacement of these fragments can be defined according to the six degrees of freedom by the translation and rotation, or planar and spherical movement of the fragments. Interfragmentary contact can be lost resulting in fragment mobility with no constant position.

The well-known posttraumatic "dish face" deformity is due to a gross retrodisplacement (in fact, it is a posterior and inferior translational movement combined with a backward tilting rotation) of major midface fragments of Le Fort II or III type, though displacement has not been originally addressed in the Le Fort system.[21] The analysis of displacement in single-piece zygoma fractures was developed quite far (translation and medial or lateral rotation around a vertical, "yaw," or longitudinal axis, "roll") to predict stability after closed reduction[33–36] and later studied in relation to a spatial xyz coordinate system to predict the ideal hardware application for reconstruction of load paths.[37]

Displacement can assume extreme proportions with complete loss of contact between minor and even major fragments due to distraction, as exemplified in zygoma and NOE fractures (►**Figs. 7–10**). If interfragmentary contacts are maintained amongst the plate- or brick-like fragments in the midfacial skeleton, countless different configurations can occur ranging from angulation, partial side shifting, to overlapping or telescoping.

In an attempt to assimilate the whole spectrum of midface and craniofacial fractures analogous to the universal AO tripartition concept of fracture classification in the human skeleton[38]—which represents a hierarchical ranking scale of fracture severity—displacement was used as the prime category to define the three basic fracture

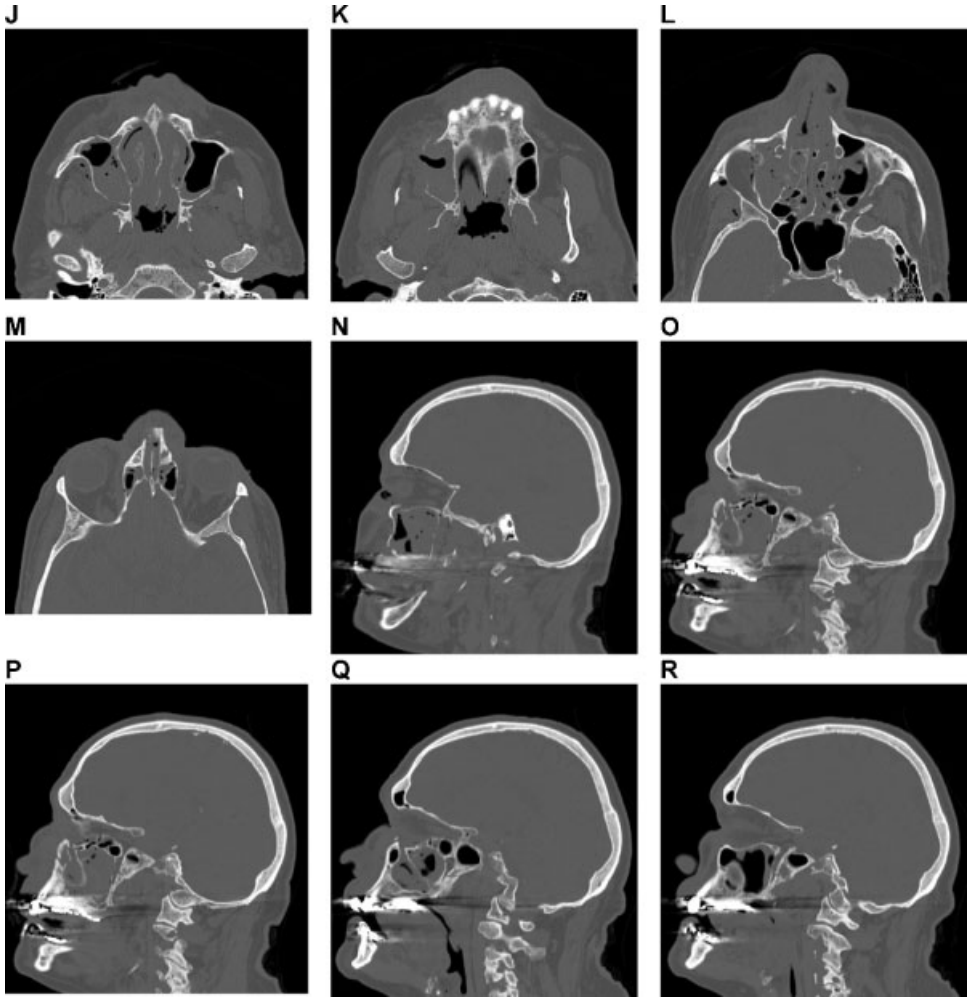


**Figure 6** (*Continued*) (J–M) axial CT scans; (N) sagittal CT scans—at lateral lamina of pterygoid process right, (O) at medial lamina of pterygoid process right, (P) at medial lamina of pterygoid process left, (Q) at lateral lamina of pterygoid process left, and (R) at lateral orbital rim left.

types before going into groups and subgroups. The distance of displacement to distinguish nondisplaced from displaced fractures was indicated as more than 2 mm. If there were several intermediate fragments with no contact between main fragments or if osseous defects greater than 5 mm were present, the fractures were considered complex.

As a consequence, fracture complexity was not defined by displacement as a uniform descriptor, but mixed with fragmentation and bone loss, overly in a somewhat arbitrary fashion. Although Le Fort and many of his successors (e.g., Markowitz et al and Jackson[8,39]) were presumptively aware that displacement of midface fractures should be measured or quantified, it was not included in classification systems.

The level 3 Midface Module considers displacement in a simple dichotomous manner (nondisplaced vs. displaced without indicating a magnitude) that can be documented in all major constituents of the central and lateral midface. The difficulty in developing a standardized instrument for qualifying or, in particular, quantifying displacement in the midface needs apprehension and admittedly requires ongoing efforts in the future because it is resolved here in a rudimentary style only.

This level 3 Midface Module deals with the dentition status and alveolar process atrophy in the maxilla as two clinically relevant items for refined description of the preinjury condition. The applied scheme for dental status is purposely limited to record the presence or absence of teeth (►**Figs. 9** and **11**). It omits dental details such as fillings, crown, and bridgework or dental pathology because these conditions go beyond pure radiographic description and require clinical assessment. Up to now enosseous dental implants remain unconsidered.

The degree of alveolar atrophy separately can be registered in the tooth gaps or overall in the maxillary processes. Likewise, as in the mandible the atrophy of the maxillary alveolar processes is typically more advanced in the posterolateral region than anteriorly in the canine and incisor region, as molars and premolars are usually lost earlier (►**Fig. 7**). In a partially edentulous alveolar process division of the upper jaw, the bony atrophy principally progresses in the same manner as in complete edentulism. Commonly,

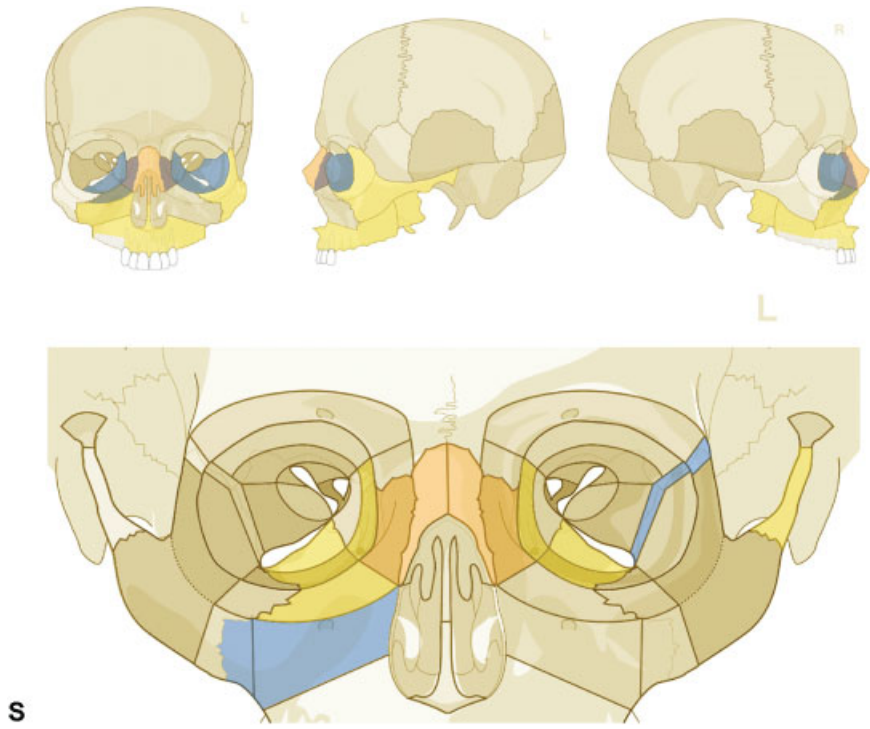


**Figure 6** (*Continued*) (S) Level 3 Code : 92 I0i.L0.Pt0.Oim.U1m.Omil.Pt0.L0.Z0, Orbit (right): R(im).W1(im)2(i), Orbit (left): R(lm).W1(lm)2(i), This case example CMTR-92-101 is made available electronically for viewing using the AOCOIAC software at www.aocmf.org/classification. Narrative description: Le Fort analogous midface fracture (central right—types I and II/centrolateral left types I and III). Unilateral NOE fracture right—large fragments, multifragmentation of facial antral wall right, nasal skeletal fracture (multifragmanted and displaced) involving both frontonasal processes and nasal bones not reaching cranially to the nasofrontal suture. Partial Dentition (FDI): Lack of 18–14; 24–28. Maxillary alveolar process atrophy: moderate. Pterygoids: bilateral incomplete horizontal fractures, no pterygomaxillary disjunction, i.e., vertical separation. Displacement: No retrodisplacement of both maxillae, no displacement of the Le Fort I and III fragments left, multifragmentation facial antral wall right, minor displacement of frontonasal fragment right. Internal orbits: Involvement confined to anterior and midorbit sections: right, medial and inferior walls, left medial, inferior and lateral walls.

the vertical atrophy is not as accentuated adjacent to remaining teeth or in tooth gaps. In addition to external atrophy of the alveolar crests, the airspaces of the maxillary sinuses expand from above into the edentulous alveolar bone of the posterior maxilla leading to continuous pneumatization and internal hollowing of the bone.[16] That is why the vertical bony atrophy in edentulism of the maxillary alveolar processes needs a synoptic assessment of the residual tooth pattern, the externally visible height of the alveolar ridge, and the degree of internal aeration. In the posterior maxilla, coronal CT scan sections are most appropriate for the evaluation of the height of the alveolar ridge relative to the extent of the maxillary sinus (distance between the alveolar crest and floor of the maxillary sinus). The vertical dimension of the alveolar ridge in the anterior maxilla (distance between the crest and the nasal floor) is best assessed in sagittal CT scan sections.

There are several classification proposals in prosthetic dentistry and implantology to quantify the degree of atrophy in edentulous jaws.[40–44] In conformity with the provisions made there, the metric value ranges to describe the three different degrees of maxillary alveolar ridge in this level 3 classification system have been selected.

In addition to the vertical atrophy, the bone dimensions of edentulous portions of the maxilla decrease in a transverse or horizontal direction.[45,46] Presumably, this three-dimensional atrophy is a predisposing factor for additional palatal fracture involvement in Le Fort type fractures. Likewise, during Le Fort I osteotomies of the edentulous upper jaw transverse fractures with a predilection site along the junction between the horizontal plate of the palatine bone and the posterior maxillary shelf were reported more frequently than in normal dentate maxillae.[47]

The broad category of tooth injuries captured in the proposed system[17] can be broken down into a manifold of subcategories (e.g., tooth loosening vertical height and horizontal crown or root fractures at different levels, infractures, extrusion, lateral luxation, etc.); however, such distinctions may only become important for individual dental treatment decisions and exceed the requirements of a more general CMF classification. To determine the degree of tooth loosening due to trauma of the periodontal supporting structures by indirect radiographic criteria is likely to be more erroneous than by simple clinical testing. Tooth avulsion, tooth loss, or missing teeth can be easily recognized, as radiographs show an empty socket.

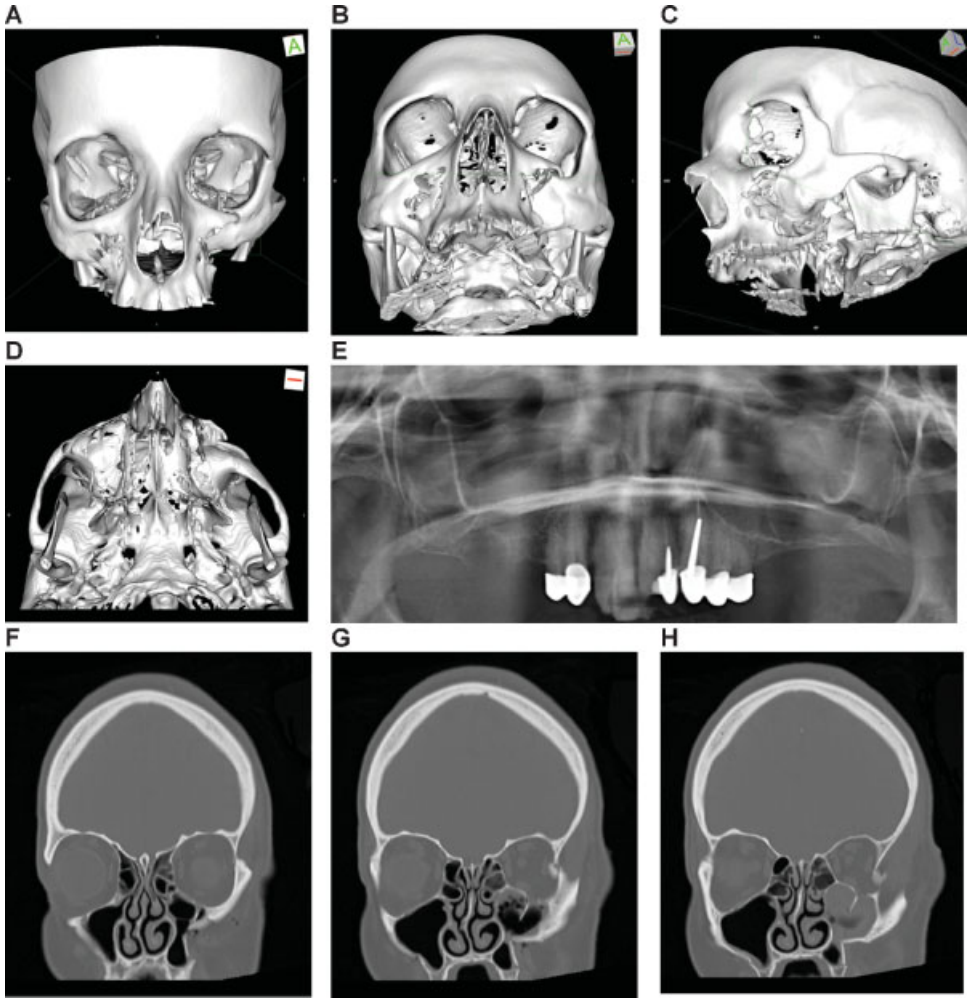


**Figure 7** Zygoma Fracture left with dorsocranial displacement and antral impaction. Three-dimensional (3D) computed tomographic (CT) scans—(A) frontal view, (B) caudofrontal view, (C) oblique lateral view left, (D) caudolateral view; panoramic X-ray—(E) OPT.

Undoubtedly, it is far more convenient to assess the dental status and dental or periodontal injuries in panoramic X-rays or Cone Beam CTs than in helical CT scans.

Fractures of the tooth-bearing alveolar processes in the two maxillae are documented as blocks specified by the incorporated teeth (►**Fig. 11**). Fracture involvement of edentulous alveolar process portions is marked in approximation to prior tooth position. It is essential not to confuse alveolar process fractures with similar fracture configurations such as unilateral Le Fort I analogous fractures or block fractures of the premaxilla reaching into the piriform aperture (i.e., floor of the nose) and into the anterior palatal shelf.[32] Horizontal fracture lines along the palatal side produced by the alveolar block must not be interpreted as true palatal fractures. Alveolar process fractures may share some of their fracture lines with adjoining fractures. The tips of the tooth roots may be completely enclosed within the fractured block, or they may protrude over the fracture line or even be snapped off and left stuck in the bony base cranial to the fractured block. In the latter case, any associated root fracture has to be registered. This is similar to the mandible level 3 classification system.[14]

Fractures of the central midface encompass all fractures located between the nasofrontal suture line and the maxillary alveolar processes with the exception of the zygomas.[26] The level 2 midface classification system divides the central midface into three horizontal partitions labeled LCM, ICM, and UCM.[2] Midface fractures commonly run through several levels in an asymmetric arrangement between the facial halves. These distinctions go back to the classification systems of Guérin,[48] Le Fort,[18,20] and Wassmund.[49] In addition to these topographical classifications, this level 3 classification system allows documentation of fragmentation and bone loss. If fracture lines cross the borders of any regions, they are assigned to all of them and marked as fragmented or nonfragmented. There are no transitional zones in between the partitions, as they were defined in the level 3 mandible classification module.[15]

The nasal skeleton is represented within the UCM including the upper septum, whereas the lower septum is included within in the LCM. Fractures of the nasal skeleton occur either

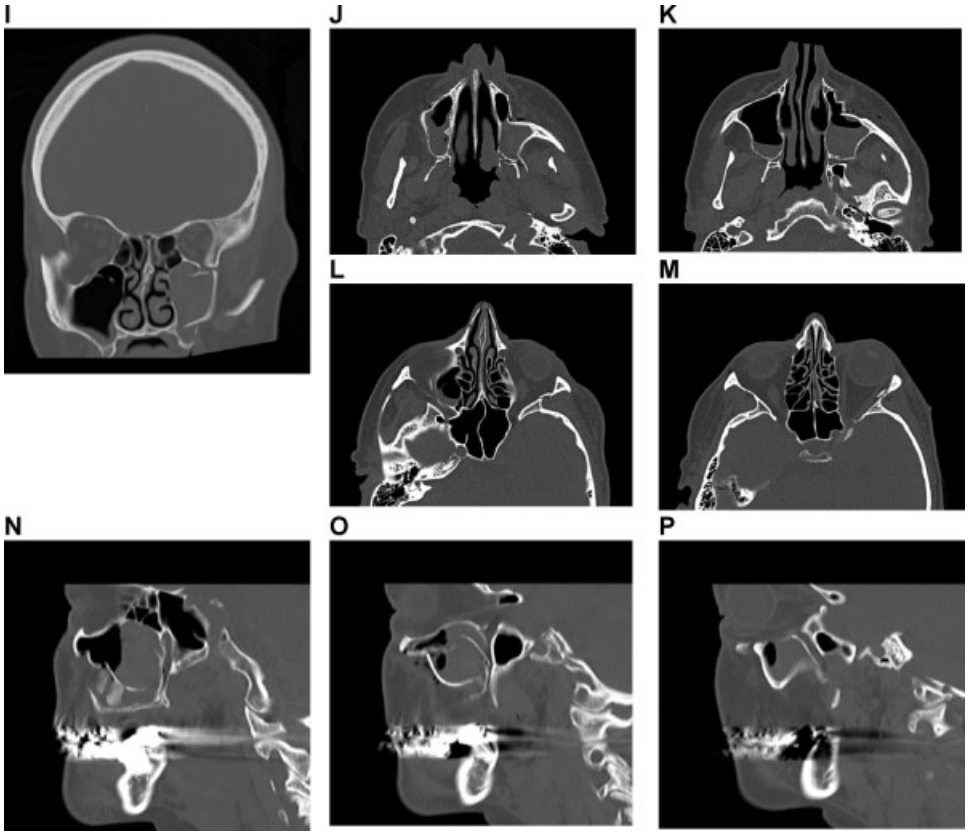


**Figure 7** (*Continued*) (F–I) coronal CT scans; (J-M) axial CT scans: sagittal CT scans—(N) next to medial orbit wall left, (O) at the level of medial orbital floor left, (P) just medial to inferior orbital fissure left.

isolated or in connection with Le Fort II and III fractures or NOE fractures (►**Figs. 8** and **9**). Traditional nasal fracture classifications employ the direction (frontal vs. lateral, cranial vs. caudal), the magnitude of the traumatic impact to the nasal vault and/or the nasal septum, the location in successive frontal planes, and concurrent injuries as the essential criteria for a categorization into different types (e.g., Stranc and Robertson, Murray et al, and Pollock[4,50,51]) In accordance with recent proposals,[52–56] a pure radiographic–morphologic evaluation is proposed here, specifying the exact location by indicating the UCM subregion (left, right, and bilateral) and/or nasal septum (upper and/or lower portion). Fragmentation can be recorded within the UCM in the presence of multiple fracture lines.

In NOE fractures, the extent of injury going beyond the nasal skeletal components into the ethmoid sinuses and the medial orbital walls including the nasolacrimal ducts must be clearly delineated. Existing classification systems concentrate either to the degree of fragmentation and avulsion of the medial canthal ligament[8] or to the topographic extension (isolated NOE vs. NOE reaching into the adjacent regions such as the frontonasal maxilla) in association with displacement of the orbital contents, orbital dystopia, or bone loss.[24,25] This entire scope of NOE injuries can be depicted in the level 3 midface classification system in its topographic bony framework. No matter to which of the two classification archetypes is resorted to, attention must be paid to the clinical status of the medial canthal ligament.[57,58] The fragmentation within the insertion zone of the ligamentous apparatus might permit to infer whether an avulsive injury is present or not.[13] Fractures and disruption of the structures essential for internal nasal support (perpendicular ethmoid plate, vomer, and quadrangular cartilage septum including lower lateral cartilages) must not be neglected in the recordings.[14] The nasal root may be more or less severely displaced into the ethmoid or superiorly into the frontal sinus and anterior cranial fossa, respectively; this kind of displacement is not recordable in the current level 3 Midface Module and should be considered for inclusion at a later stage.

Fractures of the palatal shelves are not classified in the common Le Fort fracture categories, though René Le Fort plainly reported them in some of his experimental settings.[18–20] A critical review of the numerous classification proposals[59–64] suggests to keep fractures confined to the palatal shelves apart from block fractures of the alveolar process. The horizontal fracture line of alveolar process fractures can travel with a medial offset from the very base of the process into the palatal shelf, which is why these so-called para- or palatoalveolar fractures have been inexpediently subsumed under palatal fractures.[61,64] The level 3 Midface Module distinctly differentiates alveolar process

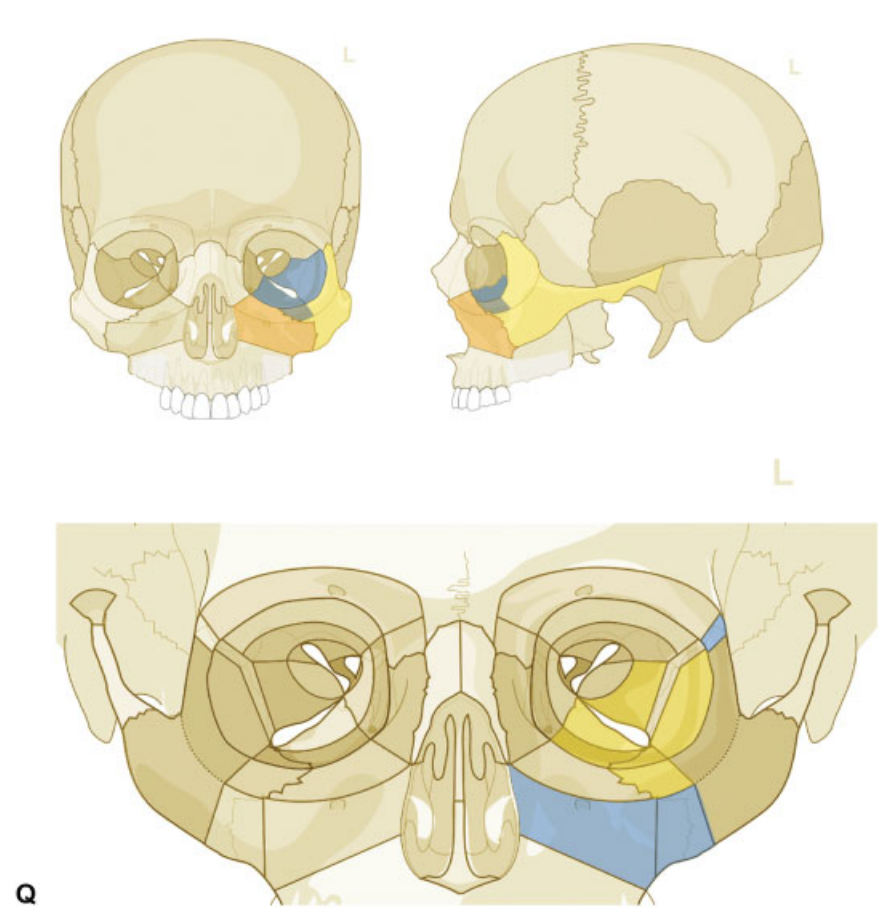


**Figure 7** (*Continued*) (Q) Level 3 Code : 92 m.Oil.I1.Z0i - 93 m.M0, Orbit (left)R(li).W1(li)2(li). This case example CMTR-92-102 is made available electronically for viewing using the AOCOIAC software at www.aocmf.org/classification. Narrative description: Zygoma fracture left. Details: fracture following ZFS, fragmentation along ZSS with intermediate fracture extending into the greater wing of sphenoid and the orbital flange of the zygoma, single fracture-infraorbital process, multifragmentation of facial antral wall left, ZMC and tuber region (LCM), zygomatic arch fracture. Dentition (FDI): Lack of 18–15; 26–28. Maxillary alveolar process atrophy: severe displacement: cranial and dorsal displacement (translational), antral impaction (rotation around sagittal axis through zygomatic body). Internal orbit left: Involvement confined to anterior orbital section and midorbit—anterolateral inferior and lateral fragments in juxtaposition to inferior orbital fissure.

from parasagittal fractures of the palatal platform (►**Fig. 11**). Together with a few other palatal fracture categories (single transverse, single midsagittal, and more than two fracture lines) this complies with a simple but effective concept. Historically, there has never been an attempt to classify the displacement and it is not made here, too.

The pterygoid processes can be regarded as the most posterior region of the facial skeleton and as separate anatomical units. As they represent the retrotuberic continuation of the maxilla and relevant pillars in the system of vertical buttresses, they are linked to the ICM and LCM. To qualify midface fractures as classic Le Fort fractures, they must transect the pterygoid process of the sphenoid bone by definition. According to textbook descriptions before the CT imaging era, the horizontal fracture lines (e.g., Rowe and Killey, Rowe and Williams, and Dingman and Natvig[34,65,66]) lie at predetermined levels: Le Fort I fractures run through the inferior third of the pterygoid laminae, Le Fort II fractures terminate in the middle, whereas Le Fort III fractures detach the pterygoid processes at their roots from the inferior surface of the sphenoid body. Irrespective of the vertical fracture level of the three classic Le Fort fracture types, the lower portion of the process stays in connection to the maxilla.[67] This contiguity is responsible for the retrodisplacement in central midface fractures due to the pull of the medial pterygoid muscle inserting in the pterygoid fossa at the back.

Fracture lines running vertically along the pterygomaxillary fissure lead to a disjunction of the pterygoid processes from the maxillae (LCM/ICM). In this condition, the intact pterygoid processes act as a natural obstacle to posterior displacement of the maxillae. Because of technical constraints in imaging, only rudimentary attempts to classify pterygoid process fractures have been made in traumatology.[68–73] Some systematic insights were gained, however, from postoperative CT scans following Le Fort I orthognathic surgery procedures and its implications on the pterygoid

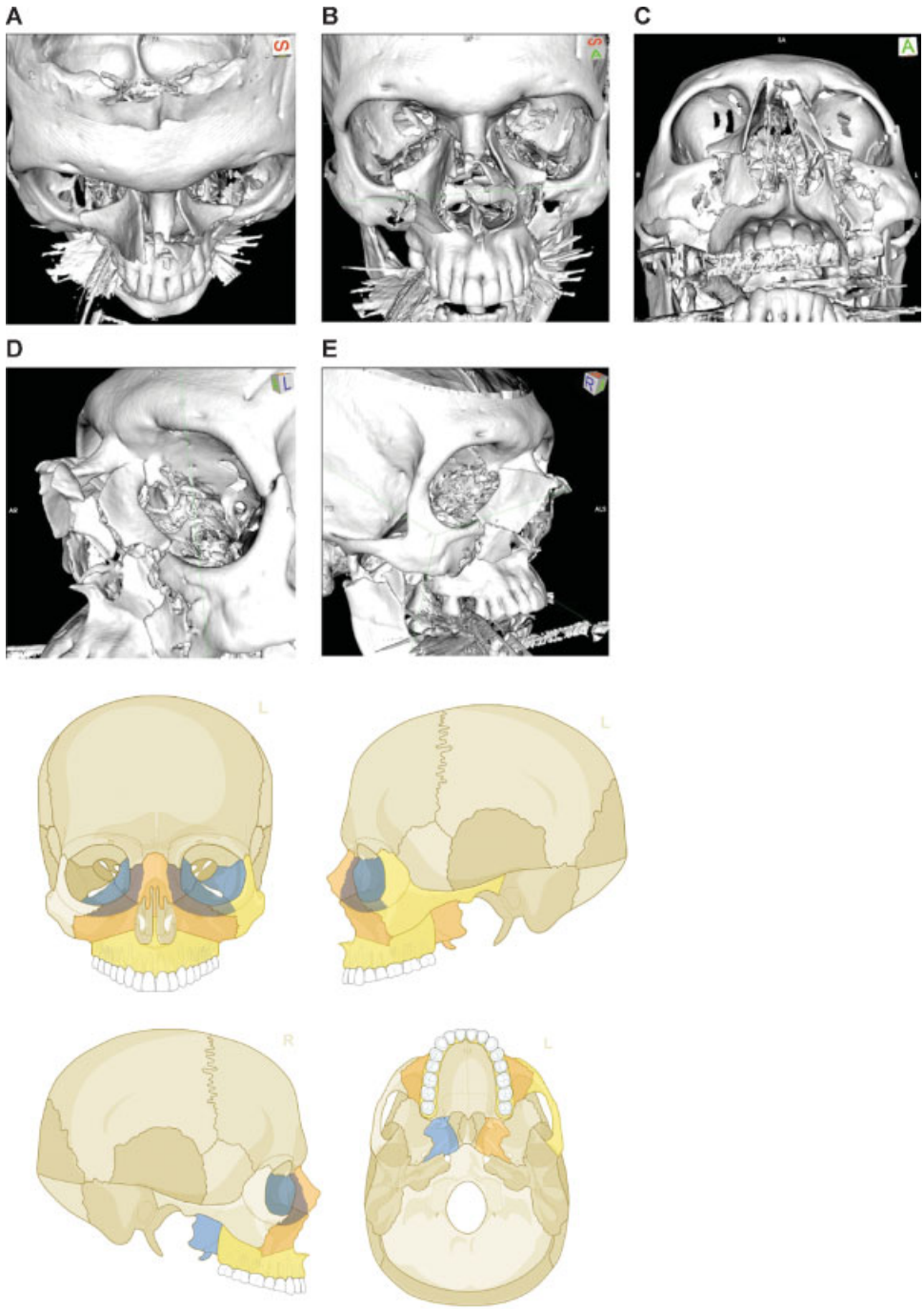


**Figure 8** Naso-orbito-ethmoidal fracture bilateral (Example 1). Imaging: Three-dimensional (3D) computed tomographic (CT) scans (A) upper frontal view, (B) frontal view, (C) lower frontal view, (D) oblique lateral view left, and (E) oblique lateral view right. Narrative description: Displacement and large-/medium-sized fragments in a bilateral Naso Orbito Ethmoid Fracture in combination with Le Fort I, II fracture, and left zygoma fracture. Note: Exclusive involvement of midfacial structures.

process.[74–77] As the level 3 midface classification system enters a new ground with differentiation between horizontal fractures and vertical disjunction of the pterygoid process (►**Figs. 8** and **9**), a redefinition and reclassification may be necessary in the near future when exploration and information have advanced.

Several proposals were made to classify fractures of the zygoma.[27,32–35,39,65,78–80] Current CT-based classification systems relate to the energy force of the impact (low, medium, and high energy) and differentiate three or four basic categories of zygomatic fractures.[27,32,39,81]

The direction of displacement and the prediction of postoperative stability were the substantial determinants of previous classifications with the intention to decide on the suitability for closed reduction. Modern systems exclusively account for the extent (localized vs. widespread) and the

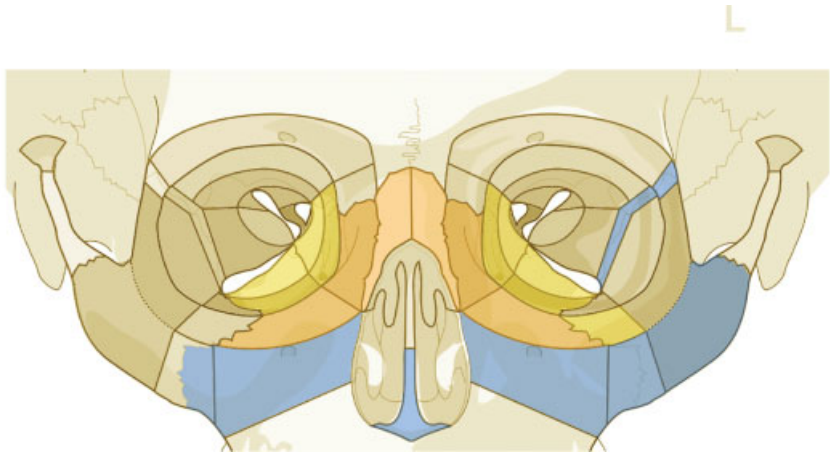


**Figure 8** (*Continued*) (F) Level 3 Code: 92 I1i.L0.Pt.Oim.U1m.Omil.Pt1.L0.I1i.Z0i, Orbit (right)R(im).W1(im)2(im), Orbit (left)R(lim).W1(lim)2 (im). This case example CMTR-92-104 is made available electronically for viewing using the AOCOIAC software at www.aocmf.org/classification.

fragmentation (en bloc/monofragment/single piece vs. multifragmentation at the articulations or throughout the entire zygoma) of the fractures.

The selection of subregions in this level 3 Midface Module allows to discern several basic zygoma fracture patterns. The proximity of the fracture line course to the anatomic suture lines and to the articulations solely or with inclusion of supplementary small-sized fragments can be indicated. Strict linear fractures often occur at the lateral orbital wall along the ZFS and ZSS, which are particularly eligible (►**Fig. 5**). The zygomaticomaxillary suture is less often separated by a single linear crack but by multiple fragments. If the ZMC and/or the zygomatic portion of the infraorbital rim are fragmented, the corresponding subregions are marked. Fragmentation within the adjacent ICM is documented by checking the ICM portion of the ZMC and/or the ICM itself according to the extent.

A nonfragmented, single-piece zygoma fracture can be unambiguously delineated from a plural-fragment zygoma fracture. A disruption at one or several of the five articulations[82] (ZFS, ZSS, infraorbital rim, zygomaticomaxillary buttress, and zygomaticotemporal sutures) is depicted by marking the subregions adjoining these interconnections as fragmented. Associated fractures of the internal orbit (blow out or blow in) need documentation as described elsewhere in this series of articles.[2] The orbital floor component of the zygoma that extends dorsally from the inferior orbital process (zygoma subdivision ID 8) must be taken into mutual account in the evaluation of orbital floor fractures.[6]

In this level 3 Midface Module, displacement is only documented as a dichotomous parameter (nondisplaced vs. displaced) referring to discontinuity of the original contours with step offs along its surfaces. These descriptors may be more refined in the future. Actually, there is a CT-based classification proposal for displacement by Fujii and Yamashiro.[83] It considers the displacement in the anteroposterior direction (*z*-axis) in 7 degrees and combines that with the 7 degrees of rotation from the X-ray-based Knight and North Classification.[33] The result is a 49-field box where one can make choices, with the most frequent displacement combinations summarized in "mainstream" subset. Such degree of complexity is most likely unnecessary for clinical practice.

Fractures of the zygomatic arch occur in isolation or as part of zygoma or Le Fort III fractures. Sometimes the zygomatic arch is intact and hinging the otherwise fractured zygoma anteriorly. In major midface trauma, the zygomatic arch is an acknowledged guide to redefine the sagittal projection of the zygoma.[67,84] Isolated zygomatic arch fractures usually present as a clinical entity of minor severity leading to contour depression at the lateral cheek and trismus due to a v-shaped indentation of the fragments toward the coronoid process. Bilateral isolated zygomatic arch fractures, however, are associated with skull or skull base fractures and an ominous sign for serious injury.[85] The majority of zygoma fracture classifications[27,33–35,39,65,80] list up isolated zygomatic arch fractures as a particular category but do not go into further details such as the exact location, nor do they outline the state of the zygomatic arch in combined fractures. Recent classification proposals address the number of fracture lines and/or the magnitude of displacement with or without residual contact between the fragments accounting for five[86] or eight[87] different fracture types.

This level 3 classification system is versatile enough to exhibit the features of the whole range of existing zygomatic arch fracture classifications and to indicate the fracture location to the midportion or to the temporal origin. A more exact location of fractures within the zygomatic arch cannot be described in the present module. The posterior aspect of the arch accommodates the roof of the glenoid fossa. It is important to distinguish fractures traversing this area in a vertical (coronal) or a sagittal ("shearing" fracture) (Fig. 7 in Kunz et al[2]) course for a precise reconstruction of the facial width and sagittal projection.

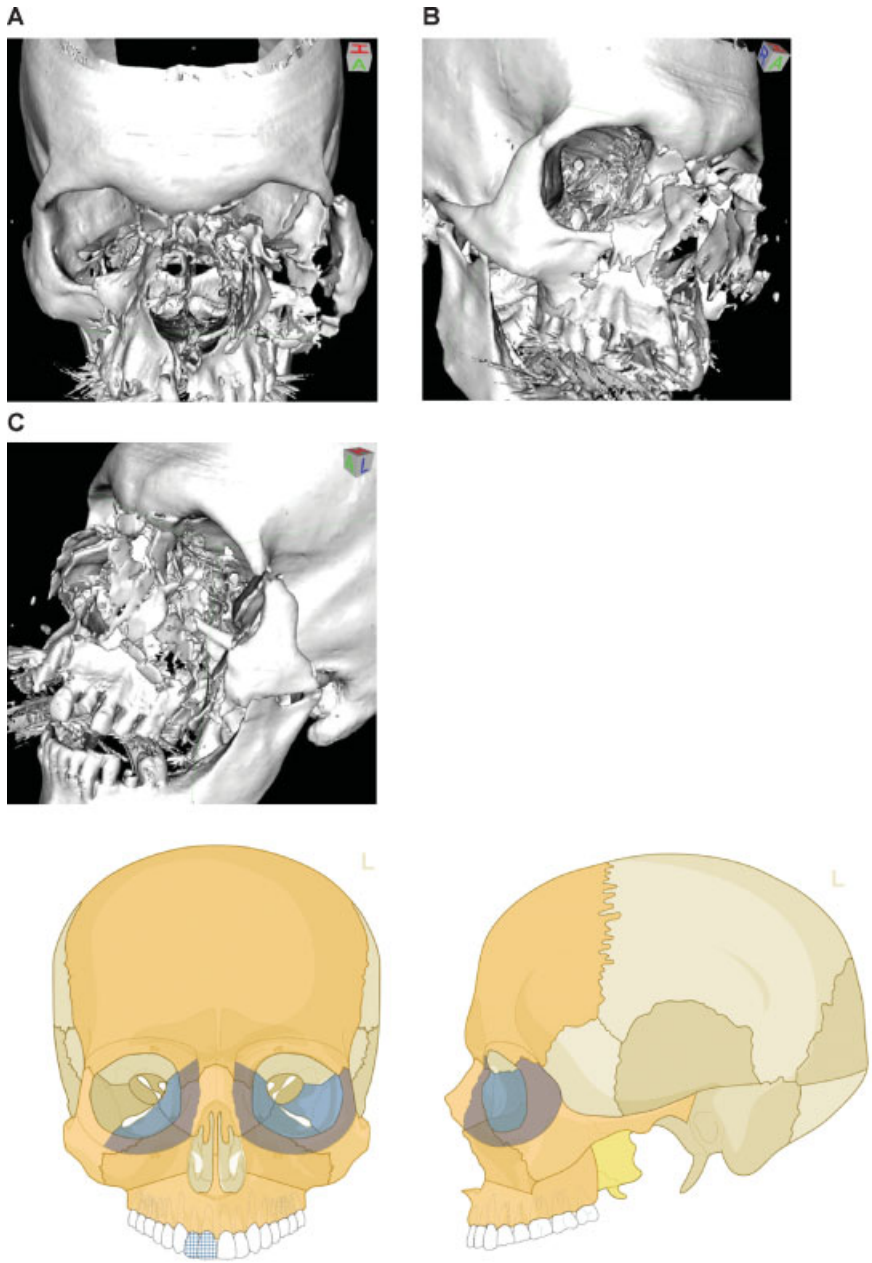


**Figure 9** Naso-orbito-ethmoidal fracture (Example 2)—NOE extreme Type III bilateral. Imaging: Three-dimensional (3D) computed tomographic scans (A) frontal view, (B) oblique lateral view right, and (C) oblique lateral view left. Narrative description: Medium-/small-sized fragments and extreme displacement (loss of interfragmentary contact) in a bilateral Naso Orbito Ethmoid Fracture in combination with a Le Fort I, II fracture, and left zyogma fracture.

Craniofacial fractures involve bones within or overlapping both sides of the junction between the viscerocranium and neurocranium, that is, the cranial base consisting of the ethmoid, sphenoid, frontal bone (frontal sinus and orbital roofs), and the clivus.

Various terminology, such as frontobasal, frontofacial, frontal sinus, frontocranial fractures, and according classifications are in common use for a topographical assignment.[23,67,88–94] The association of (subcranial) midface fractures and cranial base and/or cranial vault fractures can be captured in the level 3 classification system (►**Fig. 10**).

As the name implies, panfacial or pancraniofacial fractures involve the entire facial skeleton (►**Fig. 11**). All bony regions and subregions are affected concurrently with coexistence of the whole spectrum of midface + mandible or mandible + midface + skull base/cranial vault fractures in a multitude of different combinations.

To assign all the fractured regions and subregions of an extreme panfacial or pancraniofacial fracture into the necessary Level-3 schemes of this AOCMF classification might be ending up in a task of Sissyphean proportions, however it is possible.

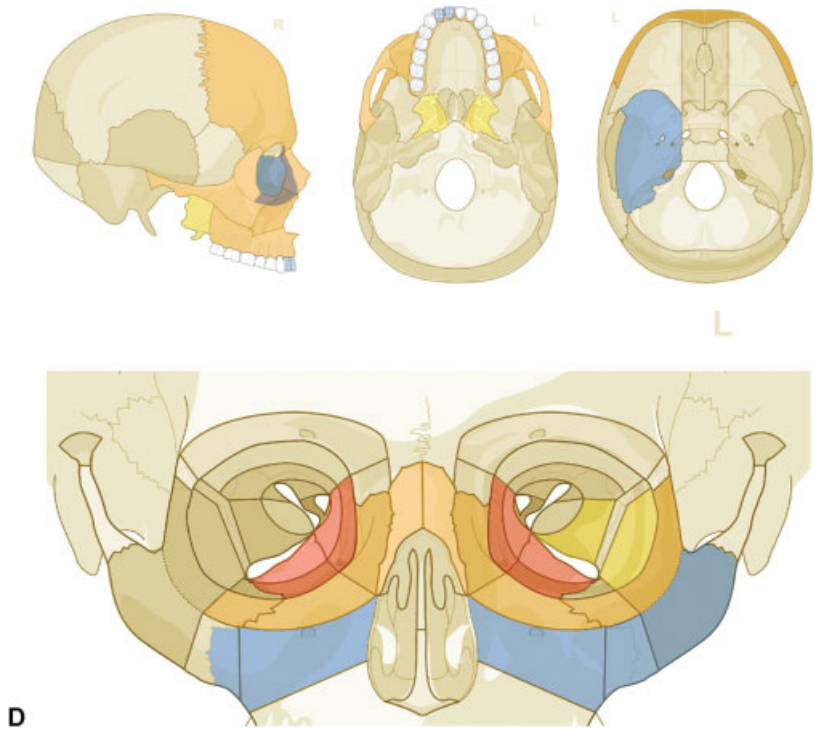


**Figure 9** (*Continued*) (D) Level 3 Code: 92 Z1i.I1i.L1.Pt0.Oim.U1m.Omil.Pt0.L1.I1i.Z1li - 93 m.M - 94 F1.m.F1m, Orbit (right): R(im).W1(im)2(im), Orbit (left): R(lim).W1(lim)2(lim). This case example CMTR-92-105 is made available electronically for viewing using the AOCOIAC software at www.aocmf.org/classification. Note: Involvement of midface and craniofacial transition as a consequence of fractures extending into the superomedial quadrants of the orbital rim - this is indicated by the marking of the entire frontal bone area.

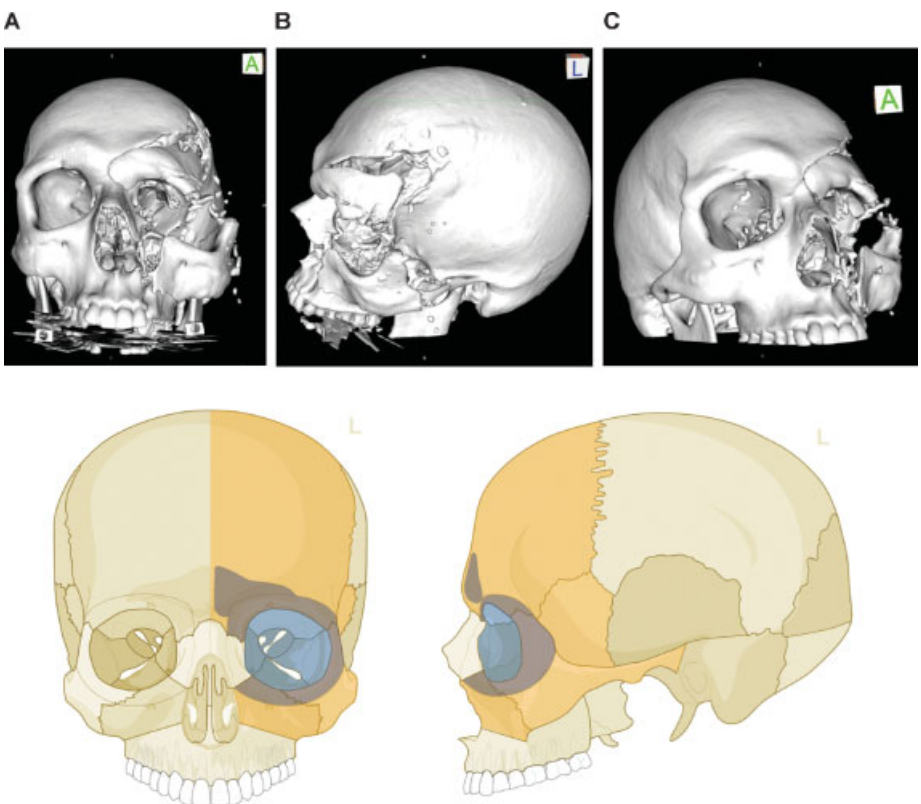


**Figure 10** Lateral cranio-orbito-facial Injury: fronto-spheno-zygomatico-orbital fracture. Imaging: Three-dimensional (3D) computed tomographic scans (A) frontal view, (B) lateral view left, and (C) oblique lateral view right. Narrative description: Large-sized fragment of left frontotemporal vault and skull base including all four orbital walls. Displaced (caudolateral) monofragment of left zygoma in continuity with infraorbital rim and antral wall, leading to an extreme diastasis of left lateral orbital wall, multifragmentation along the posterior articulations of the zygoma and in the frontotemporal transition (greater wing of sphenoid).

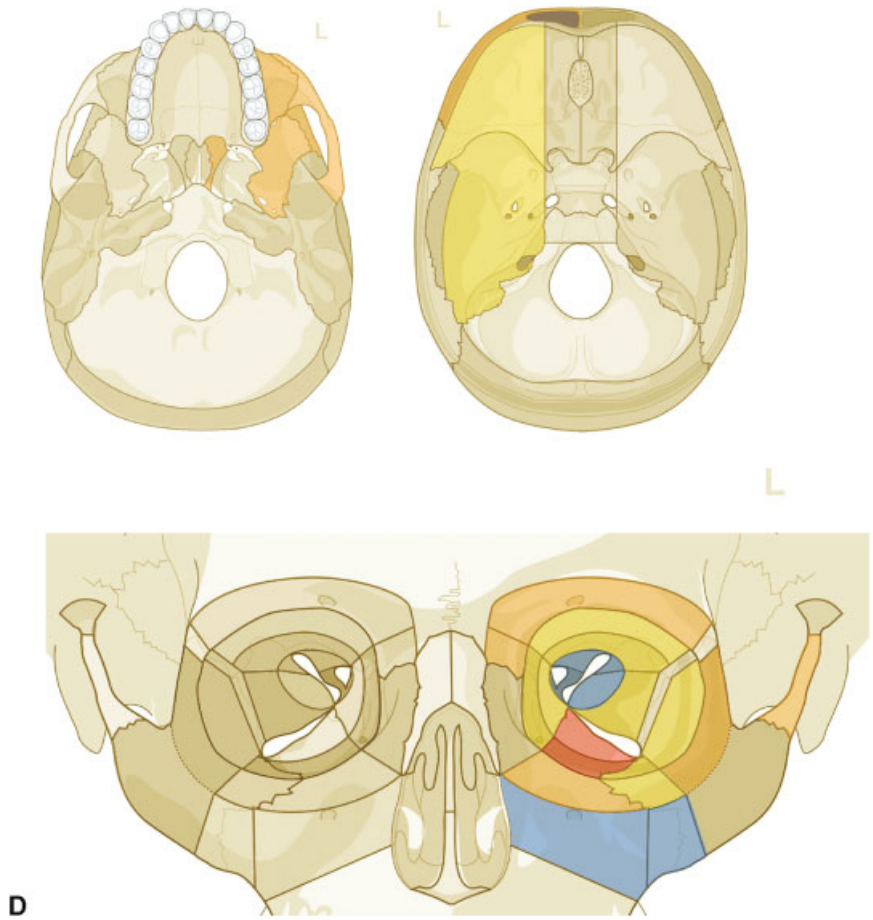


**Figure 10** (*Continued*) (D) Level 3 Code: 92 m.Omil.I1i.Z1li - 93 m.Oas.M0.A0.S1 - 94 m.F1m, Orbit (left): R(slim).W1(slim)2(slim).A(slm). This case example CMTR-92-106 is made available electronically for viewing using the AOCOIAC software at www.aocmf.org/classification.

It is anticipated that issues will be experienced with the application of this level 3 Midface Module in its current AOCOIAC version 4.0 by different users. For instance, questions will raise on how to differentiate zygoma fractures associated with multifragmentation of the antral wall (≈ ICM) from Le Fort analogous fractures exhibiting a multifragmentaton in the identical location; or what it means if a fragmentation grade 1 is assigned to all the subregions of the zygoma/zygomatic arch ensemble; or how to record an intermediate fragment of the lateral orbital wall that is located posteriorly, anteriorly, or spreading entirely over it.

A multitude of midface fracture configurations will be converted into a meaningful level 3 classification just by intuition; others will need a predefinition and algorithms that will come up in the multicenter agreement studies[1]; and eventually there may be a critical subset requiring a redesign of the classification scheme from the ground up, if it turns out clinically relevant.

Ironically enough, it is possible to display midface fracture patterns in the graphics that do not exist in reality. So far, AOCOIAC does not allow for filtering and a plausibility check of such "nonsense"—fracture combinations; however, a clear distinction must be drawn between absurdities and rarities.

## Case Examples

A series of three case examples illustrates the recording and coding of representative midface fractures:

- Asymmetric Le Fort Type midface fracture: analogous to type I level bilateral, types II and III unilateral (►**Fig. 6**).
- Dorso-cranially displaced zygoma fracture with antral impaction (►**Fig. 7**).
- Naso-orbito-ethmoidal fracture (Example 1) (►**Fig. 8**).
- Naso-orbito-ethmoidal fracture (Example 2)—extreme type bilateral (►**Fig. 9**).
- Lateral cranio-orbital facial injury: fronto-spheno-zygomatico-orbital fracture (►**Fig. 10**).
- LCM fracture analogous to Hemi Le Fort I fracture (as component of a panfacial fracture) (►**Fig. 11**).

Additional case examples are presented in a case collection appendix in this special issue.[95] Buitrago-Téllez et al[96] provide detailed information and discussion about imaging issues in this coding process.

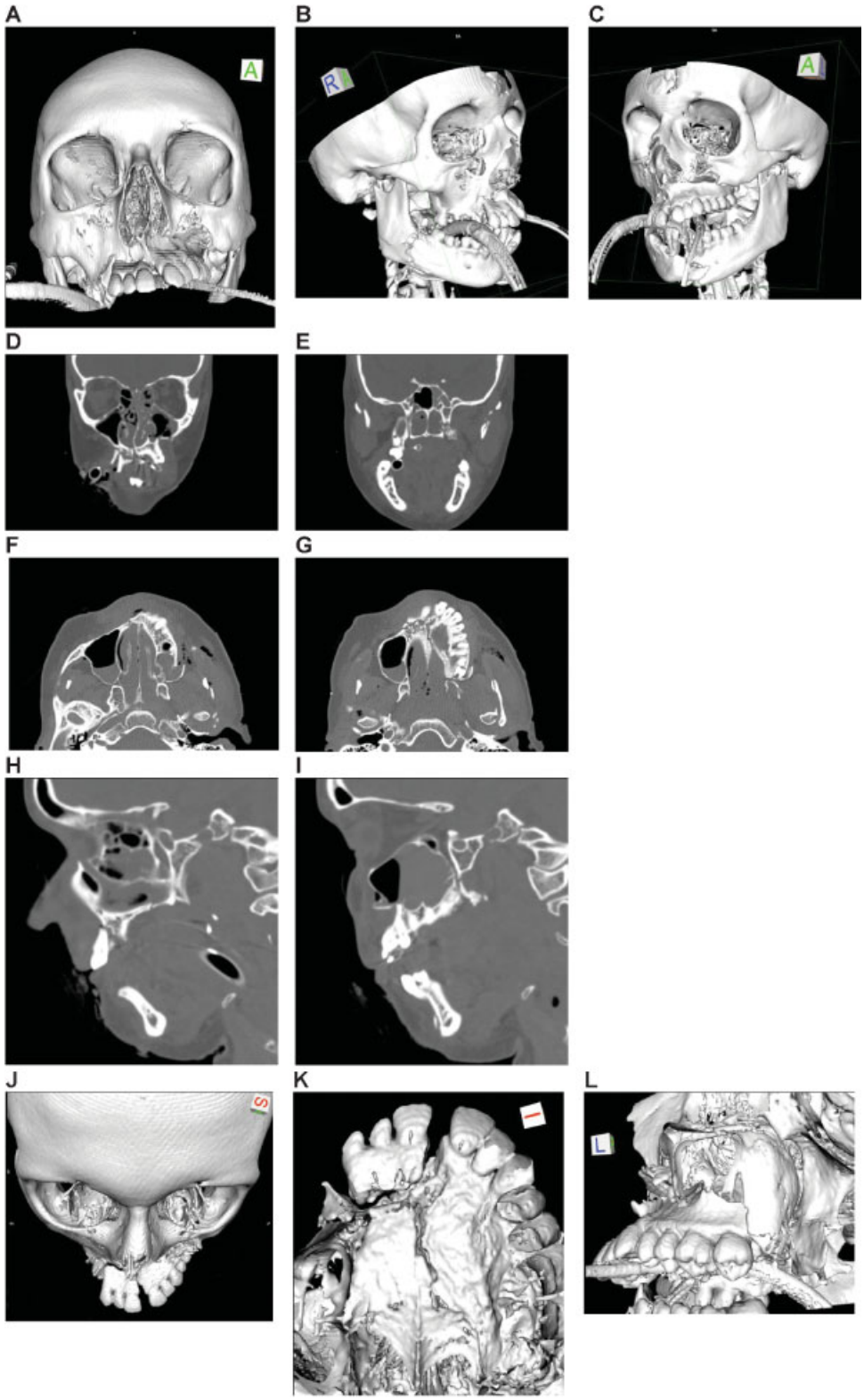


**Figure 11** Panfacial fracture including lower central midface fracture analogous to Hemi Le Fort I fracture. Imaging: Three-dimensional (3D) computed tomographic (CT) scans—(A) frontal view, (B) oblique lateral view right, (C) oblique lateral view left, (D, E) coronal CT scans; (F, G) axial CT scans; (H, I) sagittal CT scans; 3D CT scan details—(J) superofrontal view, (K) palatal from below, (l) pterygomaxillary junction. Narrative description: Midface component of panfacial fracture: LCM fracture left, paramedian midline fracture of the palate; left maxillary alveolar process fracture 11–13, vertical tooth fracture 14, avulsion 15. Details: Dentition (FDI) preinjury: completely dentate. Palate: Paramedian fracture left. Pterygoids: No involvement. Displacement: Anterosuperior displacement of the LCM fragment left, multifragmentation of the antral wall left, Infraorbital rim left intact. Internal orbits: No involvement.

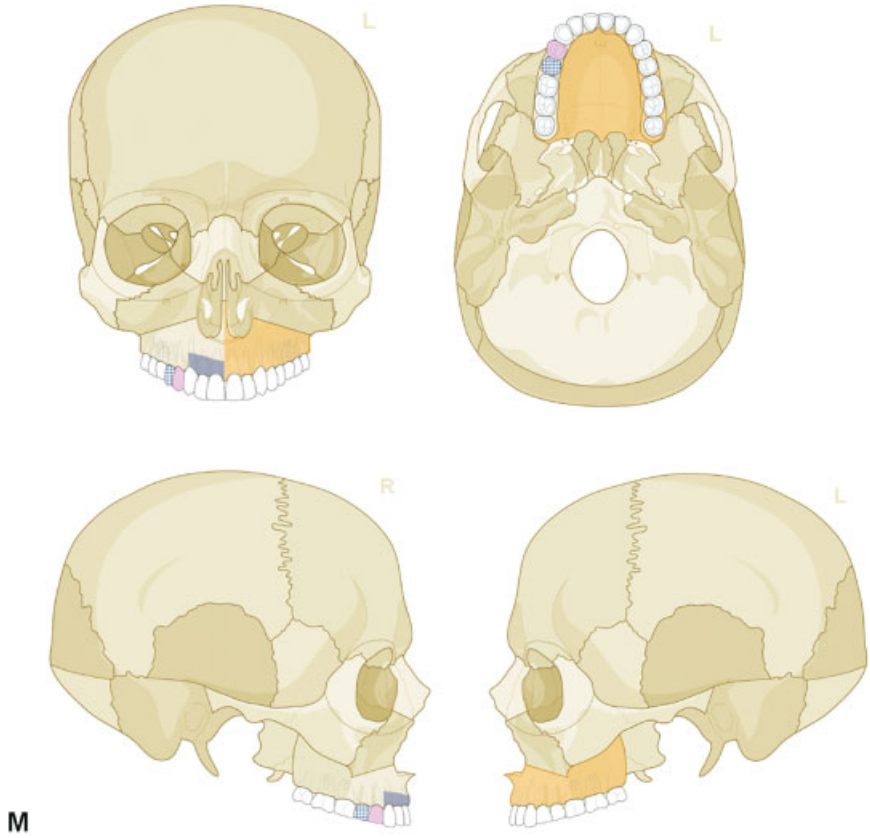


**Figure 11** (*Continued*) (M) Level 3 Code : 91 P.A.S.P - 92 La.P2.L1. This case example CMTR-92-103 is made available electronically for viewing using the AOCOIAC software at www.aocmf.org/classification. Mandible component according to level 2: four fracture regions: condylar process bilaterally, right angle/ramus and symphyseal region. Mandible component according to level 2: four fracture regions: condylar process bilaterally, right angle/ramus and symphyseal region.

## Conclusion

This level 3 Midface Module allows for a meticulous anatomical delineation of the most common fracture patterns in the midface and a description of the fracture morphology. Comparable classification concepts are pursuing to create severity scales for facial fractures introducing scores and multipliers based on the fracture morphology, soft tissue involvement treatment variables (e.g., operating time and hardware costs),[97–102] and even postoperative adverse sequelae.[103] As outlined in the introduction to this series of articles,[1] a first conception of a classification system should refer exclusively to the depiction of an injury, in particular when it is image/CT based. To carry out extrapolations on the trauma, severity necessitates retraceable correlations to a multitude of variables and factors such as bone quantity and quality, associated soft-tissue damage, functional impairment, age, physical or psychic comorbidities, quality-of-life issues and social reintegration, what imposes considerable constraints to a simple data acquisition, and reproducible documentation. This classification system represents a major step toward standardization and documentation of simple to complex midface injuries. This will hopefully foster a better understanding of the individual mapping of fractures that is necessary to establish a detailed treatment plan for a patient.

Acknowledgments

This CMF classification project was funded by the AO Foundation and its AOCMF Specialty. Illustrations were prepared by AO Education (publishing) by Jecca Reichmuth and her colleagues. The authors are grateful to all surgeons, as listed in the introduction paper of this series,[1] who participated in the successive classification sessions and provided their fruitful support in the development and validation of this mandibular fracture classification system.

## References

1 Audigé L, Cornelius CP, Di Ieva A, Prein J; CMF Classification Group. The first AO classification system for fractures of the craniomaxillofaxial skeleton: rationale, methodological background, developmental process and objectives. Craniomaxillofac Trauma Reconstr 2014;7(Suppl 1):S6–S14
2 Kunz C, Cornelius CP, Prein J, et al. The comprehensive AOCMF classification system: midface fractures - level 2 tutorial. Craniomaxillofac Trauma Reconstr 2014;7(Suppl 1):S59–S67
3 Stranc MF. Primary treatment of naso-ethmoid injuries with increased intercanthal distance. Br J Plast Surg 1970;23(1):8–25
4 Stranc MF, Robertson GA. A classification of injuries of the nasal skeleton. Ann Plast Surg 1979;2(6):468–474
5 Audigé L, Cornelius CP, Buitrago-Téllez CH, et al. The comprehensive AOCMF classification system: classification and documentation within AOCOIAC software. Craniomaxillofac Trauma Reconstr 2014;7(Suppl 1):S114–S122

6 Kunz C, Audigé L, Cornelius CP et al. The comprehensive AOCMF classification system: orbital fractures - level 3 tutorial. Craniomaxillofac Trauma Reconstr 2014;7(Suppl 1):S92–S102
7 Gullane PJ, Gilbert RW. Approach to naso-frontal-ethmoidal complex fractures. J Otolaryngol 1985;14(2):132–135
8 Markowitz BL, Manson PN, Sargent L, et al. Management of the medial canthal tendon in nasoethmoid orbital fractures: the importance of the central fragment in classification and treatment. Plast Reconstr Surg 1991;87(5):843–853
9 Fedok FG. Comprehensive management of nasoethmoid-orbital injuries. J Craniomaxillofac Trauma 1995;1(4):36–48
10 Hammer B. Orbital fractures. Diagnosis, Operative Treatment, Secondary Corretions. Seattle Toronto Bern: Hofgrefe & Huber; 1995
11 Sargent LA, Rogers GF. Nasoethmoid orbital fractures: diagnosis and management. J Craniomaxillofac Trauma 1999;5(1): 19–27
12 Sargent LA. Nasoethmoid orbital fractures: diagnosis and treatment. Plast Reconstr Surg 2007;120(7, Suppl 2):16S–31S
13 Fraioli RE, Branstetter BF IV, Deleyiannis FW. Facial fractures: beyond Le Fort. Otolaryngol Clin North Am 2008;41(1):51–76, vi
14 Vora NM, Fedok FG. Management of the central nasal support complex in naso-orbital ethmoid fractures. Facial Plast Surg 2000;16(2):181–191
15 Cornelius CP, Audigé L, Kunz C, et al. The comprehensive AOCMF classification system: mandible fractures - level 3 tutorial. Craniomaxillofac Trauma Reconstr 2014;7(Suppl 1):S31–S43
16 Ulm CW, Solar P, Gsellmann B, et al. The edentulous maxillary alveolar process in the region of the maxillary sinus—a study of physical dimension. Int J Oral Maxillofac Surg 1995;24(4): 279–282
17 Andreasen J, Cornelius CP, Gellrich N, et al. Surgery: Dentoalveolar. Foundation. Available at: http://www.aosurgery.org/dentoalveolar. Accessed August 24, 2014
18 Le Fort R. Étude expérimentale sur les fractures de la machoire supérieure (Part l). Rev Chir 1901;23:208–227
19 Le Fort R. Étude expérimentale sur les fractures de la machoire supérieure (Part ll). Rev Chir 1901;23:360–379
20 Le Fort R. Étude expérimentale sur les fractures de la machoire supérieure (Part III). Rev Chir 1901;23:479–507
21 Tessier P. The classic reprint. Experimental study of fractures of the upper jaw. Parts I and II. René Le Fort, M.D. Lille, France (Rev. chir. de Paris 23, 208–227, 360–379, 1901). Plast Reconstr Surg 1972;50(5):497–506
22 Tessier P. The classic reprint. Experimental study of fractures of the upper jaw. Part III. René Le Fort, M.D. Lille, France (Rev. chir. de Paris 23, 479–507, 1901). Plast Reconstr Surg 1972;50(6): 600–607
23 Sturla F, Abnsi D, Buquet J. Anatomical and mechanical considerations of craniofacial fractures: an experimental study. Plast Reconstr Surg 1980;66(6):815–820
24 Gruss JS. Naso-ethmoid-orbital fractures: classification and role of primary bone grafting. Plast Reconstr Surg 1985;75(3): 303–317
25 Gruss JS, Mackinnon SE. Complex maxillary fractures: role of buttress reconstruction and immediate bone grafts. Plast Reconstr Surg 1986;78(1):9–22
26 Schwenzer N, Krüger E. Midface fractures. Classification, diagnosis and fundamentals of treatment. In: Krüger E, Schilli W, eds. Oral and Maxillofacial Traumatology. 2nd ed. Chicago, IL: Quintessence Publishing Company; 1982:107–136
27 Zingg M, Laedrach K, Chen J, et al. Classification and treatment of zygomatic fractures: a review of 1,025 cases. J Oral Maxillofac Surg 1992;50(8):778–790
28 Donat TL, Endress C, Mathog RH. Facial fracture classification according to skeletal support mechanisms. Arch Otolaryngol Head Neck Surg 1998;124(12):1306–1314
29 Wanyura H. [Clinical and anatomopathologic classification of fractures of the orbit]. Rev Stomatol Chir Maxillofac 1998; 99(2):80–87
30 Yaremchuk MJ. Orbital deformity after craniofacial fracture repair: avoidance and treatment. J Craniomaxillofac Trauma 1999; 5(2):7–16
31 Manolidis S, Weeks BH, Kirby M, et al. Classification and surgical management of orbital fractures: experience with 111 orbital reconstructions. J Craniofac Surg 2002;13(6):726–737, discussion 738
32 Manson PN, Markowitz B, Mirvis S, et al. Toward CT-based facial fracture treatment. Plast Reconstr Surg 1990;85(2):202–212, discussion 213–214
33 Knight JS, North JF. The classification of malar fractures: an analysis of displacement as a guide to treatment. Br J Plast Surg 1961;13:325–339
34 Rowe NL, Killey HC. Fractures of the Facial Skeleton. General Considerations and Classification of Mandibular Fractures. 2nd ed. Edinburgh: Churchill-Livingstone; 1968:14–24
35 Larsen OD, Thomsen M. Zygomatic fracture. I. A simplified classification for practical use. Scand J Plast Reconstr Surg 1978;12(1):55–58
36 Yanagisawa E. Symposium on maxillo-facial trauma. 3. Pitfalls in the management of zygomatic fractures. Laryngoscope 1973; 83(4):527–546
37 Rudderman RH, Mullen RL. Biomechanics of the facial skeleton. Clin Plast Surg 1992;19(1):11–29
38 Buitrago-Téllez CH, Schilli W, Bohnert M, et al. A comprehensive classification of craniofacial fractures: postmortem and clinical studies with two- and three-dimensional computed tomography. Injury 2002;33(8):651–668
39 Jackson IT. Classification and treatment of orbitozygomatic and orbitoethmoid fractures. The place of bone grafting and plate fixation. Clin Plast Surg 1989;16(1):77–91
40 Cawood JI, Howell RA. A classification of the edentulous jaws. Int J Oral Maxillofac Surg 1988;17(4):232–236
41 Eufinger H, Gellrich NC, Sandmann D, Dieckmann J. Descriptive and metric classification of jaw atrophy. An evaluation of 104 mandibles and 96 maxillae of dried skulls. Int J Oral Maxillofac Surg 1997;26(1):23–28
42 Xie Q, Wolf J, Ainamo A. Quantitative assessment of vertical heights of maxillary and mandibular bones in panoramic radiographs of elderly dentate and edentulous subjects. Acta Odontol Scand 1997;55(3):155–161
43 Sağlam AA. The vertical heights of maxillary and mandibular bones in panoramic radiographs of dentate and edentulous subjects. Quintessence Int 2002;33(6):433–438
44 Juodzbalys G, Raustia AM. Accuracy of clinical and radiological classification of the jawbone anatomy for implantation—a survey of 374 patients. J Oral Implantol 2004;30(1):30–39
45 Murakami M, Kawahata N, Nagaoka E. A three-dimensional analysis method for edentulous mandibular ridge shape. Dent Mater J 2007;26(3):429–436
46 Pietrokovski J, Starinsky R, Arensburg B, Kaffe I. Morphologic characteristics of bony edentulous jaws. J Prosthodont 2007; 16(2):141–147
47 Li KK, Stephens W. Fractures of the atrophic, edentulous maxilla during Le Fort I osteotomy. Int J Oral Maxillofac Surg 1996;25(6): 430–432
48 Guérin AF. Des fractures des maxillaires supérieurs. Arch Gén Méd 1866;2:5–13
49 Wassmund M. Frakturen und Luxationen des Gesichtsschädels. Berlin: Meusser Verlag; 1927
50 Murray JA, Maran AG, Busuttil A, Vaughan G. A pathological classification of nasal fractures. Injury 1986;17(5):338–344
51 Pollock RA. Nasal trauma. Pathomechanics and surgical management of acute injuries. Clin Plast Surg 1992;19(1):133–147

52 Rohrich RJ, Adams WP Jr. Nasal fracture management: minimizing secondary nasal deformities. Plast Reconstr Surg 2000; 106(2):266–273
53 Thiede O, Krömer JH, Rudack C, et al. Comparison of ultrasonography and conventional radiography in the diagnosis of nasal fractures. Arch Otolaryngol Head Neck Surg 2005;131(5): 434–439
54 Dingman RO, Natvig P. Surgery of Facial Fractures. Philadelphia, PA: WB Saunders; 1964:267–294
55 Hwang K, You SH, Kim SG, Lee SI. Analysis of nasal bone fractures; a six-year study of 503 patients. J Craniofac Surg 2006;17(2): 261–264
56 Han DS, Han YS, Park JH. A new approach to the treatment of nasal bone fracture: radiologic classification of nasal bone fractures and its clinical application. J Oral Maxillofac Surg 2011;69(11): 2841–2847
57 Herford AS, Ying T, Brown B. Outcomes of severely comminuted (type III) nasoorbitoethmoid fractures. J Oral Maxillofac Surg 2005;63(9):1266–1277
58 Potter JK, Muzaffar AR, Ellis E, et al. Aesthetic management of the nasal component of naso-orbital ethmoid fractures. Plast Reconstr Surg 2006;117(1):10e–18e
59 Manson PN, Shack RB, Leonard LG, et al. Sagittal fractures of the maxilla and palate. Plast Reconstr Surg 1983;72(4):484–489
60 Rimell F, Marentette LJ. Injuries of the hard palate and the horizontal buttress of the midface. Otolaryngol Head Neck Surg 1993;109(3 Pt 1):499–505
61 Hendrickson M, Clark N, Manson PN, et al. Palatal fractures: classification, patterns, and treatment with rigid internal fixation. Plast Reconstr Surg 1998;101(2):319–332
62 Park S, Ock JJ. A new classification of palatal fracture and an algorithm to establish a treatment plan. Plast Reconstr Surg 2001; 107(7):1669–1676, discussion 1677–1678
63 Chen CH, Wang TY, Tsay PK, et al. A 162-case review of palatal fracture: management strategy from a 10-year experience. Plast Reconstr Surg 2008;121(6):2065–2073
64 Pollock RA. The search for the ideal fixation of palatal fractures: innovative experience with a mini-locking plate. Craniomaxillofac Trauma Reconstr 2008;1(1):15–24
65 Rowe NL, Williams JL. Maxillofacial Injuries. Edinburgh: Churchill Livingstone ; 1985
66 Dingman RO, Natvig P. Surgery of Facial Fractures. Philadelphia, PA: WB Saunders; 1964:245–260
67 Stanley RB Jr. The zygomatic arch as a guide to reconstruction of comminuted malar fractures. Arch Otolaryngol Head Neck Surg 1989;115(12):1459–1462
68 Unger JD, Unger GF. Fractures of the pterygoid processes accompanying severe facial bone injury. Radiology 1971;98(2):311–316
69 Gentry LR, Manor WF, Turski PA, Strother CM. High-resolution CT analysis of facial struts in trauma: 1. Normal anatomy. AJR Am J Roentgenol 1983;140(3):523–532
70 Gentry LR, Manor WF, Turski PA, Strother CM. High-resolution CT analysis of facial struts in trauma: 2. Osseous and soft-tissue complications. AJR Am J Roentgenol 1983;140(3):533–541
71 Ghobrial W, Amstutz S, Mathog RH. Fractures of the sphenoid bone. Head Neck Surg 1986;8(6):447–455
72 Unger JM, Gentry LR, Grossman JE. Sphenoid fractures: prevalence, sites, and significance. Radiology 1990;175(1):175–180
73 Eriksson L, Håkansson H. Unilateral fracture of the pterygoid process. Report of a case. Oral Surg Oral Med Oral Pathol 1979; 47(2):127–130
74 Renick BM, Symington JM. Postoperative computed tomography study of pterygomaxillary separation during the Le Fort I osteotomy. J Oral Maxillofac Surg 1991;49(10):1061–1065, discussion 1065–1066
75 Precious DS, Goodday RH, Bourget L, Skulsky FG. Pterygoid plate fracture in Le Fort I osteotomy with and without pterygoid chisel: a computed tomography scan evaluation of 58 patients. J Oral Maxillofac Surg 1993;51(2):151–153
76 Lanigan DT, Loewy J. Postoperative computed tomography scan study of the pterygomaxillary separation during the Le Fort I osteotomy using a micro-oscillating saw. J Oral Maxillofac Surg 1995;53(10):1161–1166
77 Lee SH, Lee SH, Mori Y, et al. Evaluation of pterygomaxillary anatomy using computed tomography: are there any structural variations in cleft patients? J Oral Maxillofac Surg 2011;69(10): 2644–2649
78 Gillies HD, Kilner TP, Stone D. Fractures of the malar-zygomatic compound: with a description of a new X-ray picture. Br J Surg 1927;14:651–656
79 Himmelfarb R. Classification and treatment of malar fractures. Oral Surg Oral Med Oral Pathol 1968;26(6):753–758
80 Spiessl B, Schroll K. Spezielle Frakturen- und Luxationslehre. Gesichtsschädel. 1 ed. Stuttgart. New York, NY: Georg Thieme Verlag; 1972:152–173
81 Paskert JP, Manson PN, Iliff NT. Nasoethmoidal and orbital fractures. Clin Plast Surg 1988;15(2):209–223
82 Cornelius CP. Zygomatic complex fractures, zygomatic arch fractures. In: Ehrenfeld M, Manson P, Prein J, eds. Principles of Internal Fixation of the Craniomaxillofacial Skeleton-Trauma and Orthognathic Surgery. New York, NY: Georg Thieme Stuttgart; 2012:204–220
83 Fujii N, Yamashiro M. Classification of malar complex fractures using computed tomography. J Oral Maxillofac Surg 1983;41(9): 562–567
84 Gruss JS, Van Wyck L, Phillips JH, Antonyshyn O. The importance of the zygomatic arch in complex midfacial fracture repair and correction of posttraumatic orbitozygomatic deformities. Plast Reconstr Surg 1990;85(6):878–890
85 Kelamis JA, Mundinger GS, Feiner JM, et al. Isolated bilateral zygomatic arch fractures of the facial skeleton are associated with skull base fractures. Plast Reconstr Surg 2011;128(4): 962–970
86 Yamamoto K, Murakami K, Sugiura T, et al. Clinical analysis of isolated zygomatic arch fractures. J Oral Maxillofac Surg 2007; 65(3):457–461
87 Ozyazgan I, Günay GK, Eskitaşçioglu T, et al. A new proposal of classification of zygomatic arch fractures. J Oral Maxillofac Surg 2007;65(3):462–469
88 Raveh J, Vuillemin T. The surgical one-stage management of combined cranio-maxillo-facial and frontobasal fractures. Advantages of the subcranial approach in 374 cases. J Craniomaxillofac Surg 1988;16(4):160–172
89 Gruss JS, Bubak PJ, Egbert MA. Craniofacial fractures. An algorithm to optimize results. Clin Plast Surg 1992;19(1): 195–206
90 Madhusudan G, Sharma RK, Khandelwal N, Tewari MK. Nomenclature of frontobasal trauma: a new clinicoradiographic classification. Plast Reconstr Surg 2006;117(7):2382–2388
91 Manson PN, Stanwix MG, Yaremchuk MJ, et al. Frontobasal fractures: anatomical classification and clinical significance. Plast Reconstr Surg 2009;124(6):2096–2106
92 Bächli H, Leiggener C, Gawelin P, et al. Skull base and maxillofacial fractures: two centre study with correlation of clinical findings with a comprehensive craniofacial classification system. J Craniomaxillofac Surg 2009;37(6):305–311
93 Hardt N, Kuttenberger J. Craniofacial Trauma - Diagnosis and Management. Berlin Heidelberg, NY: Springer Verlag; 2010
94 Marcus JR, Erdmann D, Rodriguez ED. Essentials of craniomaxillofacial trauma Quality. St Louis, MO: Medical Publishing; 2012
95 Cornelius CP, Kunz C, Neff A et al. The comprehensive AOCMF classification system: fracture case collection, diagnostic imaging workup, AOCOIAC iconography and coding. Craniomaxillofac Trauma Reconstr 2014;7(Suppl 1):S131–S135

96 Buitrago-Téllez CH, Cornelius CP, Prein J, et al. The comprehensive AOCMF classification system: radiological issues and systematic approach. Craniomaxillofac Trauma Reconstr 2014;7(Suppl 1): S123–S130
97 Cooter RD, David DJ. Computer-based coding of fractures in the craniofacial region. Br J Plast Surg 1989;42(1):17–26
98 Bagheri SC, Holmgren E, Kademani D, et al. Comparison of the severity of bilateral Le Fort injuries in isolated midface trauma. J Oral Maxillofac Surg 2005;63(8):1123–1129
99 Bagheri SC, Dierks EJ, Kademani D, et al. Application of a facial injury severity scale in craniomaxillofacial trauma. J Oral Maxillofac Surg 2006;64(3):408–414
100 Zhang J, Zhang Y, El-Maaytah M, et al. Maxillofacial Injury Severity Score: proposal of a new scoring system. Int J Oral Maxillofac Surg 2006;35(2):109–114
101 Catapano J, Fialkov JA, Binhammer PA, et al. A new system for severity scoring of facial fractures: development and validation. J Craniofac Surg 2010;21(4):1098–1103
102 Ahmad Z, Nouraei R, Holmes S. Towards a classification system for complex craniofacial fractures. Br J Oral Maxillofac Surg 2012; 50(6):490–494
103 Rottgers SA, Decesare G, Chao M, et al. Outcomes in pediatric facial fractures: early follow-up in 177 children and classification scheme. J Craniofac Surg 2011;22(4):1260–1265